International Journal of Physical Sciences

Volume 8 Number 43 23 November, 2013
ISSN 1992-1950

Academic Journals

ABOUT IJPS

The **International Journal of Physical Sciences (IJPS)** is published weekly (one volume per year) by Academic Journals.

International Journal of Physical Sciences (IJPS) is an open access journal that publishes high-quality solicited and unsolicited articles, in English, in all Physics and chemistry including artificial intelligence, neural processing, nuclear and particle physics, geophysics, physics in medicine and biology, plasma physics, semiconductor science and technology, wireless and optical communications, materials science, energy and fuels, environmental science and technology, combinatorial chemistry, natural products, molecular therapeutics, geochemistry, cement and concrete research, metallurgy, crystallography and computer-aided materials design. All articles published in IJPS are peer-reviewed.

Submission of Manuscript

Submit manuscripts as e-mail attachment to the Editorial Office at: ijps@academicjournals.org. A manuscript number will be mailed to the corresponding author shortly after submission.

For all other correspondence that cannot be sent by e-mail, please contact the editorial office (at ijps@academicjournals.org).

The International Journal of Physical Sciences will only accept manuscripts submitted as e-mail attachments.

Please read the **Instructions for Authors** before submitting your manuscript. The manuscript files should be given the last name of the first author.

Editors

Editorial Board

Instructions for Author

Electronic submission of manuscripts is strongly encouraged, provided that the text, tables, and figures are included in a single Microsoft Word file (preferably in Arial font).

The **cover letter** should include the corresponding author's full address and telephone/fax numbers and should be in an e-mail message sent to the Editor, with the file, whose name should begin with the first author's surname, as an attachment.

Article Types
Three types of manuscripts may be submitted:

Regular articles: These should describe new and carefully confirmed findings, and experimental procedures should be given in sufficient detail for others to verify the work. The length of a full paper should be the minimum required to describe and interpret the work clearly.
Short Communications: A Short Communication is suitable for recording the results of complete small investigations or giving details of new models or hypotheses, innovative methods, techniques or apparatus. The style of main sections need not conform to that of full-length papers. Short communications are 2 to 4 printed pages (about 6 to 12 manuscript pages) in length.

Reviews: Submissions of reviews and perspectives covering topics of current interest are welcome and encouraged. Reviews should be concise and no longer than 4-6 printed pages (about 12 to 18 manuscript pages). Reviews are also peer-reviewed.

Review Process

All manuscripts are reviewed by an editor and members of the Editorial Board or qualified outside reviewers. Authors cannot nominate reviewers. Only reviewers randomly selected from our database with specialization in the subject area will be contacted to evaluate the manuscripts. The process will be blind review.
Decisions will be made as rapidly as possible, and the journal strives to return reviewers' comments to authors as fast as possible. The editorial board will re-review manuscripts that are accepted pending revision. It is the goal of the IJPS to publish manuscripts within weeks after submission.

Regular articles

All portions of the manuscript must be typed double-spaced and all pages numbered starting from the title page.

The Title should be a brief phrase describing the contents of the paper. The Title Page should include the authors' full names and affiliations, the name of the corresponding author along with phone, fax and E-mail information. Present addresses of authors should appear as a footnote.

The Abstract should be informative and completely self-explanatory, briefly present the topic, state the scope of the experiments, indicate significant data, and point out major findings and conclusions. The Abstract should be 100 to 200 words in length.. Complete sentences, active verbs, and the third person should be used, and the abstract should be written in the past tense. Standard nomenclature should be used and abbreviations should be avoided. No literature should be cited.
Following the abstract, about 3 to 10 key words that will provide indexing references should be listed.

A list of non-standard **Abbreviations** should be added. In general, non-standard abbreviations should be used only when the full term is very long and used often. Each abbreviation should be spelled out and introduced in parentheses the first time it is used in the text. Only recommended SI units should be used. Authors should use the solidus presentation (mg/ml). Standard abbreviations (such as ATP and DNA) need not be defined.

The Introduction should provide a clear statement of the problem, the relevant literature on the subject, and the proposed approach or solution. It should be understandable to colleagues from a broad range of scientific disciplines.

Materials and methods should be complete enough to allow experiments to be reproduced. However, only truly new procedures should be described in detail; previously published procedures should be cited, and important modifications of published procedures should be mentioned briefly. Capitalize trade names and include the manufacturer's name and address. Subheadings should be used. Methods in general use need not be described in detail.

Results should be presented with clarity and precision. The results should be written in the past tense when describing findings in the authors' experiments. Previously published findings should be written in the present tense. Results should be explained, but largely without referring to the literature. Discussion, speculation and detailed interpretation of data should not be included in the Results but should be put into the Discussion section.

The Discussion should interpret the findings in view of the results obtained in this and in past studies on this topic. State the conclusions in a few sentences at the end of the paper. The Results and Discussion sections can include subheadings, and when appropriate, both sections can be combined.

The Acknowledgments of people, grants, funds, etc should be brief.

Tables should be kept to a minimum and be designed to be as simple as possible. Tables are to be typed double-spaced throughout, including headings and footnotes. Each table should be on a separate page, numbered consecutively in Arabic numerals and supplied with a heading and a legend. Tables should be self-explanatory without reference to the text. The details of the methods used in the experiments should preferably be described in the legend instead of in the text. The same data should not be presented in both table and graph form or repeated in the text.

Figure legends should be typed in numerical order on a separate sheet. Graphics should be prepared using applications capable of generating high resolution GIF, TIFF, JPEG or Powerpoint before pasting in the Microsoft Word manuscript file. Tables should be prepared in Microsoft Word. Use Arabic numerals to designate figures and upper case letters for their parts (Figure 1). Begin each legend with a title and include sufficient description so that the figure is understandable without reading the text of the manuscript. Information given in legends should not be repeated in the text.

References: In the text, a reference identified by means of an author's name should be followed by the date of the reference in parentheses. When there are more than two authors, only the first author's name should be mentioned, followed by 'et al'. In the event that an author cited has had two or more works published during the same year, the reference, both in the text and in the reference list, should be identified by a lower case letter like 'a' and 'b' after the date to distinguish the works.

Examples:

Abayomi (2000), Agindotan et al. (2003), (Kelebeni, 1983), (Usman and Smith, 1992), (Chege, 1998; 1987a,b; Tijani, 1993,1995), (Kumasi et al., 2001)

References should be listed at the end of the paper in alphabetical order. Articles in preparation or articles submitted for publication, unpublished observations, personal communications, etc. should not be included in the reference list but should only be mentioned in the article text (e.g., A. Kingori, University of Nairobi, Kenya, personal communication). Journal names are abbreviated according to Chemical Abstracts. Authors are fully responsible for the accuracy of the references.

Examples:

Ogunseitan OA (1998). Protein method for investigating mercuric reductase gene expression in aquatic environments. Appl. Environ. Microbiol. 64:695-702.

Gueye M, Ndoye I, Dianda M, Danso SKA, Dreyfus B (1997). Active N2 fixation in several Faidherbia albida provenances. Ar. Soil Res. Rehabil. 11:63-70.

Charnley AK (1992). Mechanisms of fungal pathogenesis in insects with particular reference to locusts. In: Lomer CJ, Prior C (eds) Biological Controls of Locusts and Grasshoppers: Proceedings of an international workshop held at Cotonou, Benin. Oxford: CAB International, pp 181-190.

Mundree SG, Farrant JM (2000). Some physiological and molecular insights into the mechanisms of desiccation tolerance in the resurrection plant Xerophyta viscasa Baker. In Cherry et al. (eds) Plant tolerance to abiotic stresses in Agriculture: Role of Genetic Engineering, Kluwer Academic Publishers, Netherlands, pp 201-222.

Short Communications

Short Communications are limited to a maximum of two figures and one table. They should present a complete study that is more limited in scope than is found in full-length papers. The items of manuscript preparation listed above apply to Short Communications with the following differences: (1) Abstracts are limited to 100 words; (2) instead of a separate Materials and Methods section, experimental procedures may be incorporated into Figure Legends and Table footnotes; (3) Results and Discussion should be combined into a single section.

Proofs and Reprints: Electronic proofs will be sent (e-mail attachment) to the corresponding author as a PDF file. Page proofs are considered to be the final version of the manuscript. With the exception of typographical or minor clerical errors, no changes will be made in the manuscript at the proof stage.

International Journal of Physical Sciences

Table of Contents: Volume 8 Number 43, 23 November, 2013

ARTICLES

academicJournals

Vol. 8(43), pp. 1994-1999, 23 November, 2013
DOI: 10.5897/IJPS2013.4014
ISSN 1992 - 1950 © 2013 Academic Journals
http://www.academicjournals.org/IJPS

International Journal of Physical Sciences

Full Length Research Paper

Homotopy analysis method with modified Reimann-Liouville derivative for space fractional diffusion equation

Jamshad Ahmad* and Syed Tauseef Mohyud-Din

Department of Mathematics, Faculty of Sciences, HITEC University, Taxila Cantt, Pakistan.

Accepted 14 November, 2013

In this paper, we applied the homotopy analysis method (HAM) to construct the analytical solutions of the space fractional diffusion equations. The derivatives are defined in the Jumarie's fractional derivative sense. The explicit solutions of the equations have been presented in the closed form by using initial conditions. Two typical examples have been discussed. The results reveal that the method is very effective and simple. On the basis of computational work and subsequent numerical results, it is worth noting that the advantage of the homotopy analysis methodology is that it displays a fast convergence of the solution.

Key words: Analytical solution, fractional diffusion equation, Reimann-Liouville fractional derivative, homotopy analysis method.

INTRODUCTION

In recent years, analysis of fractional differential equations by different methods and techniques, which are obtained from the classical differential equations in mathematical physics, engineering, vibration and oscillation by replacing the second order time derivative by a fractional derivative of order α satisfying $0 < \alpha \leq 1$, have been a field of growing interest as evident from literature survey such as, Adomian decomposition method (Momani, 2005a; Momani and Ibrahim, 2007; Momani, 2005b), variational iteration method and modified decomposition method (Das, 2008), variational iteration method (Momani et al., 2007), generalized differential transform method (Odibat et al., 2008). Fractional derivatives provide an excellent instrument for the description of memory and hereditary properties of various materials and processes.

Recently, a new modified Riemann-Liouville left derivative is proposed by Jumarie (1993, 2006). Comparing with the classical caputo derivative, the definition of the fractional derivative is not required to satisfy higher integer-order derivative than α. Secondly, α th derivative of a constant is zero. For these merits, Jumarie modified derivative we successfully applied in the probability calculus (2009) and fractional Laplace problem (Jumarie, 2009 a, b).

The solution of a fractional differential equation is much involved. In general, there exists no method that yields an exact solution for a fractional differential equation. Only approximate solutions can be derived using the linearization or perturbation methods. The homtopy anlysis method is relatively a new approach providing an analytical approximation to linear and nonlinear problems, and is particularly valuable as tool for scientists, engineers, and applied mathematicians, because it provide immediate and visible symbolic terms of analytic solutions, as well as a numerical approximate solution to both linear and nonlinear differential equations without linearization or discretization.

In this paper, we will consider space fractional diffusion equation by homotopy analysis method. The derivatives

*Corresponding author. E-mail: jamshadahmadm@gmail.com

are understood in the modified Riemann-Liouville sense. By the present method, numerical results can be obtained with using a few iterations. The homotopy analysis method (Liao, 2003a; b) contains the auxiliary parameter $\hbar$, which provides us with a simple way to adjust and control the convergence region of solution series for large value of t. Unlike, other numerical methods are given low degree of accuracy for large values of t. Therefore, the homotopy analysis method (HAM) handles linear and inhomogeneous problems without any assumption and restriction (Liao, 2009).

Firstly, we consider a one-dimensional fractional diffusion equation considered in (Meerschaert et al., 2006):

$$\frac{\partial u(x,t)}{\partial t} = d(x)\frac{\partial^{\alpha} u(x,t)}{\partial x^{\alpha}} + q(x,t), \tag{1}$$

on a finite domain $x_L < x < x_R$ with $1 < \alpha \le 2$. We assume that the diffusion coefficient (or diffusivity) $d(x) > 0$. We also assume an initial condition $u(x,t=0) = s(x)$ for $x_L < x < x_R$ and Dirichlet boundary conditions of the form $u(x_L,t) = 0$ and $u(x_R,t) = b_R(t)$. Equation 1 uses a Riemann fractional derivative of order α .

Secondly, we consider a two-dimensional fractional diffusion equation considered in Tadjeran et al. (2006):

$$\frac{\partial u(x,y,t)}{\partial t} = d(x,y)\frac{\partial^{\alpha} u(x,y,t)}{\partial x^{\alpha}} + e(x,t)\frac{\partial^{\beta} u(x,y,t)}{\partial y^{\beta}} + q(x,y,t), \tag{2}$$

on finite rectengular domain $x_L < x < x_H$ and $y_L < y < y_H$, with fractional orders $1 < \alpha \le 2$ and $1 < \beta \le 2$, where the diffusion coefficients $d(x) > 0$ and $e(x,y) > 0$. The 'forcing' function $q(x,y,t)$ can be used to represent sources and sinks. We will assume that the fractional diffusion equation has a unique and sufficiently smooth solution under the following initial and boundary conditions. Assume the initial condition $u(x,y,t=0) = f(x,y)$ for $x_L < x < x_H$, $y_L < y < y_H$ and Dirichlet boundary condition $u(x,y,t) = B(x,y,t)$ on the boundary (perimeter) of the rectengular region $x_L \le x \le x_H$, $y_L \le y \le y_H$, with the additional restiriction that $B(x_L, y,t) = B(x, y_L, t) = 0$. In physics applications, this means that the left/lower boundary is set far away enough from evolving that no significant concentrations reach that boundary. The classical dispersion equation in two-dimensions is given by $\alpha = \beta = 2$. The values of $1 < \alpha < 2$, or $1 < \beta < 2$ model a super diffusive process in that coordinate. Equation 2 also uses Riemann fractional derivatives of order α and β.

Modified Riemann-Liouville derivative

Assume $f : R \to R, x \to f(x)$ denote a continuous (but not necessarily differentiable) function and let the partition $h > 0$ in the interval [0, 1]. Through the fractional Riemann Liouville integral

$${}_0 I_x^{\alpha} f(x) = \frac{1}{\Gamma\alpha}\int_0^x (x-\xi)^{\alpha-1} f(\xi) d\xi \, , \alpha > 0, \tag{3}$$

The modified Riemann-Liouville derivative is defined as

$${}_0 D_x^{\alpha} f(x) = \frac{1}{\Gamma(n-\alpha)}\frac{d^n}{dx^n}\int_0^x (x-\xi)^{n-\alpha} (f(\xi) - f(0))\, d\xi, \tag{4}$$

where $x \in [0,1]$, $n-1 \le \alpha < n$ and $n \ge 1$.

Jumarie's derivative is defined through the fractional difference

$$\Delta^{\alpha} = (FW-1)^{\alpha} f(x) = \sum_0^{\infty} (-1)^k \binom{\alpha}{k} f[x + (\alpha - k)h], \tag{5}$$

where $FWf(x) = f(x+h)$. Then the fractional derivative is defined as the following limit,

$$f^{(\alpha)} = \lim_{h\to 0} \frac{\Delta^{\alpha} f(x)}{h^{\alpha}}. \tag{6}$$

The proposed modified Riemann –Liouville derivative as shown in Equation 4 is strictly equivalent to Equation 6. Meanwhile, we would introduce some properties of the fractional modified Riemann –Liouville derivative in Equations 7 and 8.

(a) Fractional Leibniz product law

$${}_0 D_x^{\alpha}(uv) = u^{(\alpha)} v + u v^{(\alpha)}, \tag{7}$$

(b) Fractional Leibniz formulation

$${}_0 I_x^{\alpha}\, {}_0 D_x^{\alpha} f(x) = f(x) - f(0), 0 < \alpha \le 1, \tag{8}$$

Therefore, the integration by part can be used during the fractional calculus

$${}_a I_b^{\alpha} u^{(\alpha)} v = (uv)/_a^b - {}_a I_b^{\alpha} u v^{(\alpha)}. \tag{9}$$

(c) Integration with respect to $(d\xi)^{\alpha}$

Assume $f(x)$ denote a continuous $R \to R$ function, we use the following quality for the integral with respect to $(d\xi)^{\alpha}$

$$
{}_0I_x^{\alpha} f(x) = \frac{1}{\Gamma\alpha}\int_0^x (x-\xi)^{\alpha-1} f(\xi)\, d\xi, 0<\alpha\le 1,
$$
$$
= \frac{1}{\Gamma(1+\alpha)}\int_0^x f(\xi)(d\xi)^{\alpha}, \tag{10}
$$

HOMOTOPY ANALYSIS METHOD (HAM)

We consider the following differential equation:

$$
FD[u(x,t)] = 0, \tag{11}
$$

where *FD* is a nonlinear operator for this problem, *x* and *t* denote an independent variable, $u(x,t)$ is an unknown function. In the frame of homotopy analysis method (HAM), we can construct the following zeroth-order deformation:

$$
(1-q)L(U(x,t;q)-u_0(x,t)) = q\hbar H(x,t)FD(U(x,t;q)), \tag{12}
$$

where $q \in [0,1]$ is the embedding parameter, $\hbar \neq 0$ is an auxiliary parameter, $H(x,t) \neq 0$ is an auxiliary function, *L* is an auxiliary linear operator, $u_0(x,t)$ is an initial guess of $u(x,t)$ and $U(x,t;q)$ is an unknown function of the independent variables *x, t* and *q*.
Obviously, when $q=0$ and $q=1$, it holds respectively.

$$
U(x,t;0) = u_0(x,t), \quad U(x,t;1) = u(x,t), \tag{13}
$$

Using the parameter *q*, we expand $U(x,t;q)$ in Taylor series as follows:

$$
U(x,t;q) = u_0(x,t) + \sum_{m=1}^{\infty} u_m(x,t)\, q^m, \tag{14}
$$

Where

$$
u_m = \frac{1}{m!}\frac{\partial^m U(t;q)}{\partial^m q}\bigg|_{q=0}.
$$

Assume that the auxiliary linear operator, the initial guess, the auxiliary parameter $\hbar$ and the auxiliary function $H(x,t)$ are selected such that the series (12) is convergent at $q=1$, then due to Equation 12 we have

$$
u(x,t) = u_0(x,t) + \sum_{m=1}^{\infty} u_m(x,t) \tag{15}
$$

Let us define the vector

$$
\vec{u}_n(x,t) = \{u_0(x,t), u_1(x,t), \ldots, u_n(x,t)\}
$$

Differentiating Equations 10 *m* times with respect to the embedding parameter *q*, then setting $q=0$ and finally dividing them by $m!$, we have the so-called *m*th-order deformation equation

$$
L[u_m(x,t) - \chi_m u_{m-1}(x,t)] = \hbar H(x,t) R_m(\vec{u}_{m-1}), \tag{16}
$$

Where

$$
R_m(\vec{u}_{m-1}) = \frac{1}{(m-1)!}\frac{\partial^{m-1} FD(U(t;q))}{\partial^{m-1} q}\bigg|_{q=0},
$$

And

$$
\chi_m = \begin{cases} 0 & m \le 1, \\ 1 & m > 1. \end{cases}
$$

Finally, for the purpose of computation, we will approximate the HAM solution of Equation 9 by the following truncated series:

$$
\phi_m(t) = \sum_{k=0}^{m-1} u_k(t).
$$

NUMERICAL APPLICATIONS

In this section, we apply the proposed algorithm of homotopy analysis method (HAM) using Jumarie's approach for fractional order diffusion equation:

Example 1: We consider a one-dimensional fractional diffusion equation for Equation 1, as taken (Meerschaert et al., 2006; Ray et al., 2008):

$$
\frac{\partial u(x,t)}{\partial t} = d(x)\frac{\partial^{1.8} u(x,t)}{\partial x^{1.8}} + q(x,t), \tag{17}
$$

on a finite domain $0<x<1$, with the diffusion coefficient

$$
d(x) = \Gamma(2.2)x^{2.8}/6 = 0.183634\ x^{2.8}, \tag{18}
$$

the source/sink function

$$
q(x,t) = -(1+x)e^{-t}x^3, \quad for\ 0<x<1, \tag{19}
$$

with the initial conditions $u(x,0)=x^3$ and the boundary conditions

$$
u(0,t)=0, \quad u(1,t)=e^{-t},\ for\ t>0. \tag{20}
$$

According to Equation 12, the zeroth-order deformation can be given by

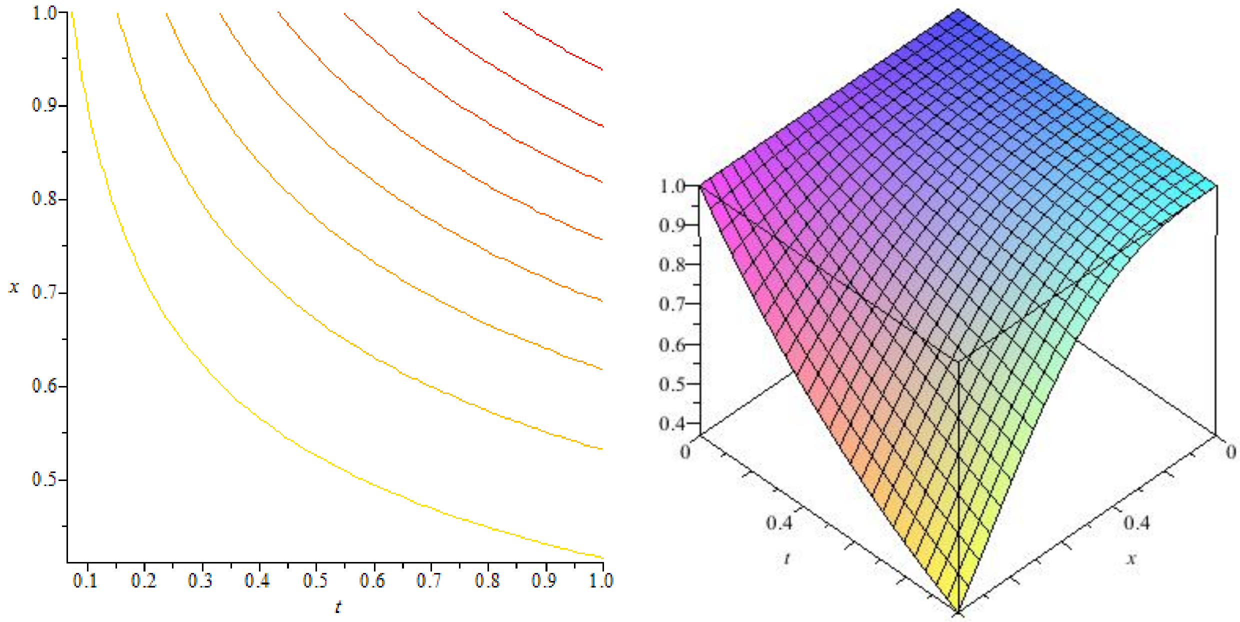

Figure 1. The surface shows the solution $u(x,t)$ for Equation 17.

$$(1-q)L\left(U(x,t;q)-u_0(x,t)\right)=q\hbar H(x,t)\left(\frac{\partial u(x,t)}{\partial t}-d(x)\frac{\partial^{1.8}u(x,t)}{\partial x^{1.8}}-q(x,t)\right), \quad (21)$$

We choose the auxiliary linear operator $L\left(U(x,t;q)\right)=D_\alpha^t U(x,t;q)$, with the property $L(C)=0$, where C is an integral constant. We also choose the auxiliary function to be $H(x,t)=1$. Hence, the *m*th-order deformation can be given by:

$$L\left[u_m(x,t)-\chi_m u_{m-1}(x,t)\right]=\hbar H(x,t)R_m(\vec{u}_{m-1}),$$

Where

$$R_m(\vec{u}_{m-1})=\frac{\partial u_{m-1}(x,t)}{\partial t}-d(x)\frac{\partial^{1.8}u_{m-1}(x,t)}{\partial x^{1.8}}-q(x,t) \quad (22)$$

Now the solution of the *m*th-order deformation Equation 14 for $m\geq 1$ become

$$u_m(x,t)=\chi_m u_{m-1}(x,t)+\hbar L^{-1}\left[R_m(\vec{u}_{m-1})\right]. \quad (23)$$

Consequently, the first few terms of the HAM series solution for $\hbar=-1$ are as follows:

$$u_0=e^{-t}x^3+e^{-t}x^4-x^4,$$

$$u_1(x,t)=(-e^{-t}+1)x^4+\frac{4(-e^{-t}+1-t)x^5}{2.2},$$

$$u_2(x,t)=\frac{4(e^{-t}-1+t)x^5}{2.2}+\frac{80(e^{-t}-\frac{t}{2!}-1+t)x^5}{3.2\times 2.2^2},$$

$\vdots$

It obvious that the noise terms appear between the components u_0 and u_1, and these are all canceled. The closed form solution is $u(x,t)=e^{-t}x^3$.

The surface (Figure 1) shows the solution $u(x,t)$ for equation (17).

Example 2: Now, we consider a two-dimensional fractional diffusion equation for Equation 2, considered in (Tadjeran et al., 2006; Ray et al., 2008):

$$\frac{\partial u(x,y,t)}{\partial t}=d(x,y)\frac{\partial^{1.8}u(x,y,t)}{\partial x^{1.8}}+e(x,t)\frac{\partial^{1.6}u(x,y,t)}{\partial y^{1.6}}+q(x,y,t), \quad (24)$$

on a finite rectengular domain $0<x<1$, $0<y<1$, for $0\leq t\leq T_{end}$ with the diffusion coefficients

$$d(x,y)=\Gamma(2.2)x^{2.8}y/6, \quad (25)$$

$$e(x,y)=2xy^{2.6}/\Gamma(4.6), \quad (26)$$

and the forcing function

$$q(x,y,t)=-(1+2xy)e^{-t}x^3y^{3.6}, \quad (27)$$

with the initial condition

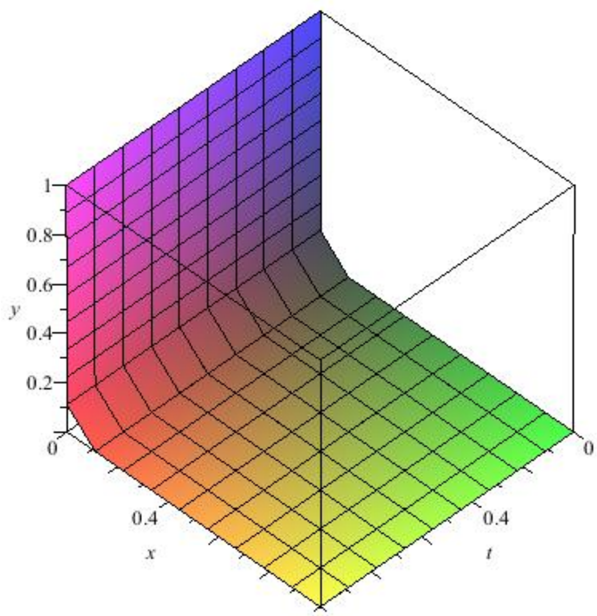

Figure 2. The surface shows the solution $u(x,t)$ for Equation 24.

$$u(x,y,0) = x^3 y^{3.6}, \tag{28}$$

and Dirichlet boundary conditions on the rectangle in the form

$$u(x,0,t) = u(0,y,t) = 0, \quad u(x,1,t) = e^{-t} x^3, \tag{29}$$

and

$$u(1,y,t) = e^{-t} y^{3.6}, \quad \textit{for all } t \geq 0. \tag{30}$$

According to Equation 12, the zeroth-order deformation can be given by

$$(1-q)L\big(U(x,t;q) - u_0(x,t)\big) = q\hbar H(x,t). \\ \left(\frac{\partial u(x,y,t)}{\partial t} - d(x,y)\frac{\partial^{1.8} u(x,y,t)}{\partial x^{1.8}} - e(x,t)\frac{\partial^{1.6} u(x,y,t)}{\partial y^{1.6}} - q(x,y,t)\right), \tag{31}$$

We choose the auxiliary linear operator $\mathrm{L}(\mathrm{U}(\mathrm{x},\mathrm{t};\mathrm{q})) = \mathrm{D}_\alpha^{\mathrm{t}}\mathrm{U}(\mathrm{x},\mathrm{t};\mathrm{q}),$ with the property $L(C) = 0,$ where C is an integral constant. We also choose the auxiliary function to be $\mathrm{H}(\mathrm{x},\mathrm{t}) = 1.$ Hence, the *m*th-order deformation can be given by:

$$L[u_m(x,t) - \chi_m u_{m-1}(x,t)] = \hbar H(x,t) R_m(\vec{u}_{m-1}),$$

Where

$$R_m(\vec{u}_{m-1}) = \frac{\partial u_{m-1}(x,y,t)}{\partial t} - d(x,y)\frac{\partial^{1.8} u_{m-1}(x,y,t)}{\partial x^{1.8}} - e(x,t)\frac{\partial^{1.6} u_{m-1}(x,y,t)}{\partial y^{1.6}} - q(x,y,t) \tag{32}$$

Now the solution of the *m*th-order deformation in Equation 14 for $m \geq 1$ become

$$u_m(x,t) = \chi_m u_{m-1}(x,t) + \hbar L^{-1}[R_m(\vec{u}_{m-1})]. \tag{33}$$

Consequently, the first few terms of the HAM series solution for $\hbar = -1$ are as follows

$$u_0 = x^3 y^{3.6} e^{-t} + 2x^4 y^{4.6} e^{-t} - 2x^4 y^{4.6},$$
$$u_1(x,t) = x^4 y^{4.6}(-e^{-t} + 1) + \left(\frac{8}{2.2} + \frac{2 \times 4.6}{3}\right) x^5 y^{5.6}(-e^{-t} + 1 - t),$$
$$u_2(x,t) = \frac{1106}{165} x^5 y^{5.6}(e^{-t} - 1 + t) + \frac{9101827}{272250} x^6 y^{6.6}(e^{-t} - 1 + t - \frac{t^2}{2!}),$$
$$\vdots$$

It obvious that the "noise" terms appear between the components u_0 and u_1, and these are all canceled. The closed form solution is $u(x,y,t) = x^3 y^{3.6} e^{-t}.$

The surface (Figure 2) shows the solution $u(x,t)$ for equation (24).

Conclusion

In this paper, the application of homotopy analysis method (HAM) was extended to obtain explicit and numerical solutions of linear and inhomogeneous space fractional diffusion equations with initial and boundary conditions. The obtained results and computational work demonstrate the reliability of the algorithm, reconform the convergence of the suggested algorithm and its wider applicability to fractional differential equations. The advantage of HAM is the auxiliary parameter which provides a convenient way of controlling the convergence region of series solutions. It is clear that the solutions agree with the exact solutions. Further, the proposed technique is fully capable of coping with the nonlinearity of such physical problems. İt may be concluded that this suggested technique is a nice addition to the existing techniques for solving nonlinear problems of diverse fields.

REFERENCES

Das S (2008). Solution of Fractional Vibration Equation by the Variational Iteration Method and Modified Decomposition Method, Int. J. Nonlinear Sci. Numerical Simulation. 9:361-365.

Jumarie G (1993). Stochastic differential equations with fractional Brownian motion input, Int. J. Syst. Sci. 6:1113-1132.

Jumarie G (2006). New stochastic fractional models for Malthusian growth, the Poissonian birth process and optimal management of populations, Math. comput. Model.44:231-254.

Jumarie G (2009a). Table of some basic fractional calculus formulae derived from a modified Riemann-Liouville derivative for non-differentiable functions, Appl. Math. Lett. 22.

Jumarie G (2009b). Laplace s transform of fractional order via the Mittag–Leffler function and modified Riemann- Liouville derivative, Appl. Math. Lett. 22:1659-1664.

Liao SJ (2003a). Beyond perturbation: Introduction to the homotopy analysis method, Chapman and Hall/CRC Press, Boca Raton.

Liao SJ (2003b). on the analytic solution of magneto hydro dynamic flows of non-Newtonian fluids over a stretching sheet. J. Fluid Mech. 488:189–212.

Liao SJ (2009). Notes on the homotopy analysis method: Some definitions and theorems Commun. Nonlinear Sci. Numer. Simulat. 14:983–997.

Momani S (2005a). An explicit and numerical solutions of the fractional KdV equation, Mathematics and Computers in Simulation, 70(2):110-118.

Momani S, Ibrahim R (2007). Analytical solutions of a fractional oscillator by the decomposition method, Int. J. Pure Appl. Mathe. 37(1):119-132.

Momani S (2005b). Analytic and approximate solutions of the space- and time-fractional telegraph equations. Appl. Mathe. Computation. 170(2):1126-1134.

Momani S , Odibat Z, Alawneh A (2007). Variational iteration method for solving the space-fractional and time- fractional KdV equation, Num. Meth. For Part. Diff. Equ. 24(1):262 -271.

Meerschaert MM, Scheffler H, Tadjeran C (2006). Finite difference methods for two-dimensional fractional dispersion equation, J.Comput. Phys. 211:249–261.

Odibat Z, Momani S, Alawneh A (2008). Analytic study on time-fractional Schrödinger equations: Exact solutions by GDTM, J. Phys. Conf. Series 96 012066.

Ray SS, Chaudhuri KS, Bera RK (2008). Application of modified decomposition method for the analytical solution of space fractional diffusion equation, Appl. Mathe. Comput. 196:294–302.

Tadjeran C, Meerschaert MM, Scheffler H (2006). A second-order accurate numerical approximation for the fractional diffusion equation, J. Comput. Phys. 213:205-213.

academicJournals

Vol. 8(43), pp. 2000-2010, 23 November, 2013
DOI: 10.5897/IJPS2013.4018
ISSN 1992 - 1950 © 2013 Academic Journals
http://www.academicjournals.org/IJPS

International Journal of Physical Sciences

Full Length Research Paper

Feasibility and technical studies of two water recirculating systems using two different power sources, solar photovoltaic and fuel generator

Oparaku N. F. and Nnaji C. E.*

National Centre for Energy Research and Development, University of Nigeria, Nsukka, Nigeria.

Accepted 5 November, 2013

Recirculating water systems are designed to minimize or reduce dependence on water exchange and flushing in fish culture units. Water is typically recirculated when there is a specific need to minimize water replacement, to maintain water quality conditions which differ from the supply water, or to compensate for an insufficient water supply. In this work, recirculating system of fish was used in rearing fish which comprised of fish ponds and treatment pond. Submersible pump was powered by solar energy while the electropome pump was powered by generator provided electricity. Simple annual costs analysis as well as net present value (NPV) method were used to compute the profitability. The total fixed cost of using recirculation system with solar powered pump was higher by ₦163, 500.00 while the total variable cost of using recirculation system with generator was higher by ₦244000.00. NPV's recorded were 299607, -66323, -40409 for generator powered system and 1336085, 575047, 626113 for solar powered system at r = 0.1, 0.2, 0.19, respectively. Results also indicated a shorter payback period for solar system. Solar as power source was more profitable than generator despite its high initial capital.

Key words: Recirculating system, solar photovoltaic, fish culture, net present value, financial feasibility, fuel generator.

INTRODUCTION

Recirculating system maximizes water re-use by employing comprehensive water treatment system. Water treatment processes typically are solid removal, infiltration, gas balancing, oxygenation, and disinfection. By addressing each of the key water concern through treatment rather than flushing as is used in flow-through and the partial reuse systems, ultimate control over culture conditions and water quality is provided.

There is growing interest in recirculation aquaculture system (RAS) technology in the world, as a result of perceived advantages over the conventional aquaculture (Emperor Aquatics, 2008; The Fish Site, 2010; Zhang et al., 2011; Food and Water Watch, 2008). Recirculating system can help in reduction of water and land usage. Recirculating system offers a high degree of control over the culture environment and fish biomass can be determined easily and accurately than in biomass. Even though it is capital intensive, claim of impressive yields with year-round production is attracting growing interest from prospective aquaculturists" (Losordo et al., 1998; Poulson, 2013; Rakacy, 2006). To evaluate the profitability of the venture, indicators of investment returns were determined such as net present value (NPV) and internal rate of return (IRR), payback period, (NAERL, 2000) and (Parin and Lupin, 1995). The operation of RAS which are mechanically sophisticated and biologically complex requires education, expertise and dedication (Duning et al., 1998). Many commercial

*Corresponding author. E-mail: chibueze.nnaji@unn.edu.ng, Tel: +234(0)8030967563.

RAS have failed because of component failure due to poor design and inferior management (Masser et al., 1999; Sioux Indian Reservation, 2006). Good knowledge of the design of the system, specification of the technical components and operation of the system is therefore a prerequisite for a sustainable RAS farm. The water treatment process could increase operation costs and failure of the treatment system would result in huge economics losses (Summerfelt et al., 2001). Therefore, the aspect of economic feasibility has to be taken into consideration before embarking on the system. Generally, a feasibility study is conducted during the planning stage prior to obtaining approval for funds or financing of a project. The study analyzes and assesses feasibility of using solar photovoltaic and generator that uses fuel. Financial feasibility and other factors that could influence the sustainability of the project. It is important to critically evaluate the outcome or conclusions of a feasibility study. A good study may uncover alternatives and save significant time and money for the stakeholder of the project. The aims and objectives were to analyze the profitability of recirculating systems powered with generator and electricity and technical feasibility of the project.

MATERIALS AND METHODS

The project was carried out between January, 2009 and December, 2009 at the National Centre for Energy research and Development, University of Nigeria Nsukka. Nsukka is located at 6.9°N and 7.4°E and 445 m above sea level.

Treatment tank installation

Procurements of biofilters namely bioblocks, biobrush, Maifan stones, coral sand, ceramic ring, activated charcoal and Ultra Violet (UV) light were used for this study. They were arranged inside the treatment tank in the following order:

Biobrush ⟶ Bioblock ⟶ Maifan stones ⟶ Coral sands ⟶ Ceramic ring and Activated Charcoal ⟶ UV light (the arrows shows the order of arrangement of the compartments of the treatment tank)

The dimensions of treatment tank which was constructed with concrete are (3.4 × 1×1.5) m. There were four compartments in the water treatment tank each measuring (1× 0.6 ×1.25) m. The first compartment contains the biobrush, the second has bioblocks, the third contains maifan stones, coral sands, ceramic ring and activated charcoal, finally the last chamber houses the UV fluorescent tube which was placed at close proximity to the water surface but was not immersed in the water. Two pumps, Interdab electropome Jet 100 M 1horse power pump and Grundfos KPBasic 300A submersible pump were procured at Onitsha and Lagos respectively. Interdab electropome Jet 100 M uses electricity while Grundfos submerssible pump was powered by solar modules (photovoltaic) to ensure constant power supply and to serve as comparative between electric and solar energy. The quantity of water pumped by both pumps is 50 L/min at the depth of 1.25 m. Air stone aerator supply oxygen constantly to the ponds. Ceramic rings - surface area 1200 m^2/L and weighing 10 kg, bamboo carbon (activated carbon) - surface area 1200 m^2/L and weighing 10 kg were purchased at Kingdom Aquarium and fisheries Ltd. Lagos, Nigeria. Two overhead plastic tanks, volume 1000 L each were procured at Onitsha for water storage.

Treatment process

Water from the overhead tank (Inlet water) entered the pond where fishes are kept and then flowed into the treatment tank as waste water. As waste water flowed through biobrush, bioblocks, maifan stone, coral sand, ceramic ring and activated carbon it is filtered. Solar powered pump water and electric powered pump water were then collected. Water lastly flowed into the UV light compartment where it was disinfected (UV treated water). After the waste water had passed through the treatment tank, the treated water was air lifted into the culture tank for use by the fish and recirculated back again into the filter again for purification.

Methods of estimating profitability of recirculating systems

The methods used for evaluating profitability were the following: Rate of return on the original investment (i_{ROI}), Present-worth (PW), Net Present Value and Pay out time (n_R) (Parin and Lupin, 1995).

Rate of return on the original investment (i_{ROI})

The annual net profit divided by total initial investment represents the fraction which, when multiplied by 100, is known as the percentage return on investment. The procedure used was to find the return on total original investment, with the value of the average net profit being the numerator and thus, the rate of return on the original investment, i_{ROI} =

$$NP_a = \frac{1}{n} \times \sum_{j=1}^{n} NP_j = \frac{NPa}{It}$$

Np_a = annual net profit , I_t = total initial investment.

Present-worth (PW)

This method compared the present-worth (PW) of all the cash flows with the original investment. It assumed equal opportunities for re-investment of the cash flows at a pre-assigned interest rate.

$$PW = \sum_{j=1}^{n} \frac{CF_j}{(1+i)^j} - I_T \quad , \quad PW' = \frac{\sum_{j=1}^{n} \frac{CF_j}{(1+i)^j}}{I_T}$$

Where, CF = cash flow; I_T = initial Investment; i = interest rate.

Net present value

The net present value (NPV) of a project is the difference between the sum of the discounted cash flows which are expected from the investment and the amount which is initially invested. A trial and error method was used to establish the interest rate to be applied to the cash flow each year, such that the original investment would be reduced to zero (or salvage value, plus land, plus working capital) during the useful life of the project. Internal rate of return, r, is calculated by trial and error:

DCFRR = IRR = r,

Table 1. Description of fixed and variable investment of using recirculating system with solar photovoltaics.

S/N	Description of fixed Investment	Unit cost	Price	Variable investment	Cost
1	Pond Construction	150,000	N150,000		
2.	Treatment Tank Construction	N80,000.00	N80,000.00	Cost of paying a labourer every month (N10000.00 a month)	N120000.00
3.	Plumping materials and connections cost	N58,000	N58,000	3500 Fingerlings at N200 each	N70,000.00
4.	Electric wiring of the pond	-	N5,000		
5.	Cost of Roofing for air pump mounting		N50,000.00	Cost of rearing a fish for 1 year- N200 x 3500	N700,000.00
6.	Grundfos water pump	N36,000.00	N36,000.00		
7.	4 Panels (100 Amps)	N55,000.00	N210,000		
8.	Charge Controller	N18,000.00	N18,000.00		
9.	Stand for the Panels	N7,000.00	N7,000.00	Annual servicing cost	N5000.00
10.	Inverter	N55,000.00	N55,000.00		
11.	UV Flourescent Tube	N36,000.00	N36,000.00		
12.	Oxygen Pump with (air stones)	N49,000.00	N49,000.00	Miscellanous	20,000.00
13.	Biobrush (4)	N1,500.00	N6,000.00		
14	Bioblocks	N27,000.00	N27,000.00	**Total variable**	**N915,000.00**
15.	Hand net for scoping the fish out of the pond	N4,000.00	N8,000.00		
16	Booth & Polythene Trouser	N10,000.00	N10,000.00		
17.	Water analysis kit	N40,00.00	N40,000.00		
18.	2 Battery (12v)	N25,000	N50,000.00		
19.	Ground Artermia (one tin)	N9,000.00	N9,000.00		
20.	Grinding mill(3Horse power)		N55,000.00		
21.	20 packets of Coral Sands (1000 g)	N1,000.00	N20,000		
22.	20 packets of activated carbon(500 g)	N1,000.00	N20,000		
	Total fixed Cost		N1059,000.00		
	Total Cost		N1974000.00		

where $$\sum_{j=1}^{n}\frac{CF_j}{(1+r)^j} - I_T = 0$$

NPV typically is calculated over a specific time period of interest, e.g., 3 or 5 years. If the project NPV is greater than zero, the project is considered to be profitable over that time period. If the project NPV is less than zero, the project is considered to be not profitable over that time period.

Pay out time/Payback period

This method focus on recovering the cost of investment. Pay out time represents the amount of time that it takes for a capital budgeting project to recover its initial costs pay out time, in years = Fixed depreciable investment / (average profit/year) +(average depreciation/year).

$$Average \cdot Cash \cdot Flow = CF_a = \frac{1}{n} \times \sum_{j=1}^{n} CF_j \quad Pay \cdot out \cdot time, n_R = \frac{I_F}{CF_a}$$

$I_{F=}$ Fixed depreciable Investment; $C_{F\ =}$ average profit/year; a= average depreciation/year.

RESULTS

Methods of estimating profitability of recirculating systems

Total Cost =Total Fixed Cost (TFC) + Total Variable Cost (TVC)
Total Cost = N1059, 000.00 + N915,000.00 = N1974 000.00 (Table 1)
Total revenue= (price of 1 mature fish=N400 × 3500) = N1, 400,000.00
Annual- profit= TR-TVC = N I, 400,000 – N915, 000 = N485, 000.00

Annual cost analysis

Total Cost =Total Fixed Cost (TFC) + Total Variable Cost (TVC).
Total Cost = N895, 500.00 + N1,159, 000.00 = N2054,500 (Table 2).
Total revenue= (price of 1 mature fish=N400 × 3500) = N1, 400,000.00.

Table 2. Description of Fixed and variable Investment of using recirculating system with generator.

1.	Pond Construction (3)	N150,000	Variable Investment	Costs
2.	Treatment Tank Construction	N80,000.00	3500 Fingerlings at N20 each	N70,000.00
3.	Plumbing materials and Connection Cost	N58,000.00	Cost of rearing a fish for 1 year N200 × 3500	N700,000.00
4.	Wiring of the pond	N5,000.00	Cost of Paying a labourer per month(N10000.00) for 1 year	N120000.00
5	Cost of Roofing for air pump	N50,000.00		
6	Electric Pump	N26,000.00	Cost of fuel for 1 month N19500 (30 × 650).	N234000.00
7.	2 Generators (model 2700)	N 70,000.00		
8	UV Flourescebt Tube	N36,000.00	Cost of oil filter, oil, fuel filter, after every 600 hrs of operation (7 times a year) for a sduty cycle of 12 h / day	N 10, 000.00
9	Bioblocks (1 cubic metre)	N27,000.00		
10	4 Biobru	N6,000	Annual inspection and servicing cost	N 5000. 00
11.	Cost of 10 Brood Stocks	N10,000.00		
12.	Cost of Ovaprim	N3,500.00	Miscellanous	N20,000.00
13	Oxygen Pump with Air stones	N49,000.00	**Total variable cost**	**N1,159,000.00**
14.	Hand Net	N 8000.00		
15.	Bo oth and Polythene Trouser	N10,000.00		
16.	Pelleting machine	N104,000.00		
17.	Water kit Analysis	N40,000.00		
18.	Cost of ground Artermia (one tin)	N8,000.00		
19.	Grinding machine	N55,000.00	**Total Cost**	**N2,054,500.00**
	Filter Media	N20,000		
20.	20 packets of Maifan Stones	N20,000		
	20 Ceramic Rings	N20,000.00		
21	20 packets of Coral sands	N 20,000.00		
22	20 packets 0f bamboo (activated charcoal)	N20,000.00		
	Total fixed cost	**N 895500.00**		

Annual profit = TR-TVC =N 1, 400,000 – N1,159,000 = N241, 000.00

(i) The total fixed cost of using recirculation system with solar powered pump is higher by (N1059, 000.00 – N895, 500.00) =N163, 500.00

(ii) The total variable cost of using recirculation system with generator is higher by (N1159000.00 – N915, 000.00) = N244000.00 (cost of fuel for 1 year) (Table 2).

Decision

Adopting any of the recirculation system is profitable. However, it is more profitable to adopt recirculation system with solar powered pump since the 1 year variable cost (raw materials + labour) was lowered by N244, 000.00. The cost of a generator (model 2700) was N35000 (Table 3), salvage value of generator was N10, 000 while the useful life was put at 5 years, depreciation

Table 3. Statement of sources and application of funds for a for a recirculating system using generator.

Activity	2005	2006	2007	2008	2009	2010	2011	2012	2013	2014
Capital	N2,054,500									
Working capital	N1159,000									
Applications										
Fixed investment	N895500.00									
variable cost	1159000.00	1159000	1159000	1159000.00	1159000	1159000	1159000.00	1159000	1159000	1159000
Total revenue	1,400,000	1400,000	1400,000	1400,000	1400,000	1,400,000	1400,000	1,400,000	1400,000	1400,000
Costs of production	1159000	1159000	1159000	1159000	1159000	1159000	1159000	1159000	1159000	1159000
Annual profit	241,000	241000	241000	241000	241000	241,000	241000	241000	241000	241000
Minus 10% tax	48200	48200	48200	48200	48200	48200	48200	48200	48200	48200
Net profit	192800	192800	192800	192800	192800	192800	192800	192800	192800	192800
Plus depreciation	5000	5000	5000	5000	5000	5000	5000	5000	5000	5000
Cash flow	197800	197800	197800	197800	197800	197800	197800	197800	197800	197800

value was N5000.00. The salvage value of solar panels was N15000.00 and useful life was 25 years, depreciation was put at N6, 400.00. A tax assumed to be levied on the fish produced was 20% per annum and was deducted from the annual gross profit. Operating costs include fixed costs and variable costs. Fixed costs are associated with the long-term operation of a catfish farm. Examples include: taxes (on property), insurance, depreciation, interest, amortization payments (for repayment of borrowed money). These costs are often overlooked but must be considered in assessing the financial situation of a catfish farm. Variable costs are the costs that vary with the size of the catfish farm or the number of ponds being stocked. Larger farms (or stocking more ponds) have much greater total variable production costs than smaller farms. Examples include: feeds, seed/fingerlings, fuel and/or power, chemicals, fertilizers, harvesting costs, and labour. Expected returns include the money that the catfish farmer receives from the sale of catfish. Profit is the most important return and is determined by subtracting the costs of production from the amount received when the catfish are sold. (Note: start-up costs, annual fixed costs, and variable production costs must all be used in calculating production costs). Returns from catfish farming may be reported as “gross” or “net” returns –the distinction between the two is important.

Gross return refers to the total amount of money received for the catfish that are sold. Not much consideration is given to how much it cost to produce the crop. Gross return is calculated by multiplying the total number of kilograms sold by the price received per kilogram for the fish. Net return refers to the total amount of money remaining after all costs of production have been subtracted from gross returns. Net return is also known as profit.

It is a more important measure of a catfish farm than gross return. Net return also reflects on the efficiency of the catfish farm. These costs and returns were summarized in table form (Tables 3 and 4).

Rate of return on the original investment

The percentage return on original investment for recirculating system that uses solar photovoltaic was 36.6% while that of generator was 21.5% the time value of money was not considered, since only the average profit was used, not its timing. Recirculating system with solar is the best in terms of profitability because the value of rate of return on original investment was greater than values in the generator. The profits from years 1 through 10 could be reversed and the return on original investment would be the same.

The present-worth

The present-worth and the PW' relationship for the recirculating system was calculated by applying a rate of i = 15% per year in equation, the following results were obtained for generator powered recirculating system: The result for the present worth was N3713 and photovoltaic was

Table 4. Statement of sources and application of funds for a recirculating system using photovoltaics as power source.

Activity	2005	2006	2007	2008	2009	2010	2011	2012	2013	2014
Capital	N1,974,000									
Working capital	N915,000									
Applications										
Fixed investment	N1,059,000									
Variable costs	915,000	915,000	915,000	915000	915,000	915,000	915,000	915,000	915,000	915,000
New battery procurement after three years				50,000						
Total Revenue	1,400,000	1400,000	1400,000	1400,000	1400,000	1,400,000	1400,000	1,400,000	1400,000	1400000
Costs of production	915,000	915,000	915,000	965,000	915,000	915,000	915000	915,000	915000	915000
Annual Gross profit	485,000	485000	485000	435000	485000	485000	485000	485000	485000	485000
Minus 10% tax	97000	97000	97000	97000	97000	97000	97000	97000	97000	97000
Net profit	388,000	388,000	388,000	348,000	388,000	388,000	388,000	388,000	388,000	388,000
Plus depreciation	6400	6400	6400	64000	6400	6400	6400	6400	6400	6400
Cash flow	394400	394400	394400	354400	394400	394400	394400	394400	394400	394400

N8146296. At the end of ten years, the cash flow to the project, compounded on the basis of end-of-year income, will be: for generator empowered recirculating system, F = N93303 For photovoltaics empowered recirculating system; F = N8146296 . The relationship between the present-worth of the annual cash flow and the total capital investment for generator was PW' = 988803/ 895500 = 1.1042, for photovoltaics was PW' = $8146296 / 1059000 =$ 7.692.

Net present value (NPV)

Net present values recorded were 299607, -663232, -40409 at r = 0.1, 0.2, 0.19, respectively for the generator powered recirculating system. NPV values for photovoltaics powered recirculating system were as follows 1336085, 575047, 626113 at r = 0.1, 0.2 and 0.19, respectively. Net present values recorded were positive for photovoltaic systems while it is positive at r =0.1 in generator powered system (Tables 5 and 6).

However, solar as power source was more profitable than generator. It is the present value of future net cash inflows minus the initial capital cost. Each year's net cash flows can be reduced by the present value by multiplying it by $\frac{1}{(1+r)}$ where r = interest and n is the year considered. This process is known as discounting. The present values of all the annual net cash flows can then be summed up to give the total present value. If the initial investment is subtracted from the total present value, the result is called the net present value (NPV).

Discounted cash flow rate of return

The values calculated for r = 0.15 and 0.2, respectively for photovoltaic and generator, the resulting rate of return calculated (Figures 1 and 2) was equivalent to the maximum interest rate that could be paid to obtain the necessary funds to finance the investment and completely paid back by the end of the useful life of the project. The interpolation to determine the correct value of r was done by plotting the relationship between the original investment and the total present-worth as a function of r, as is shown in Figures 3 and 4.

Planning farm operations

The profitably model was used to plan the cash flows over the 10 year planning horizon. The investment and finance schedule indicated how much finance the farmer needed (equity plus loan), interests, repayment and depreciation (depreciation needed for tax calculation). The operations statement showed the net profits after

Table 5. Calculation of internal rate of return for the recirculating system of fish pond powered by generator.

Year (m)	Cash flow (Naira) d_m	Trial for r = 0.1		Trial for r = 0.2		r = 0. 19	
		Factor	Present-worth (Naira)	Factor d_m	Present-worth (Naira)	Factor d_m	Present-worth (Naira)
0	(895500)						
1	197800	0.909	178020	0.833	164767	0.840	166152
2	197800	0.826	163383	0.694	137273	0.705	139449
3	197800	0.751	148548	0.579	114526	0.592	117098
4	197800	0.683	135097	0.482	95340	0.497	98307
5	197800	0.621	122834	0.402	79515	0.417	82483
6	197800	0.564	111559	0.335	66263	0.350	69230
7	197800	0.513	101471	0.279	55186	0.294	58153
8	197800	0.466	92175	0.232	45890	0.247	48857
9	197800	0.424	83667	0.194	38373	0.207	40945
10	197800	0.385	76153	0.162	32044	0.174	34417
Total			1195107		829177		855091
Relationship = Total present-worth / Original investment			$\frac{1195107}{895500}$ =1.3346		$\frac{829177}{895500} = 0.9260$		$\frac{855091}{895500}$ =0.9549
NPV			299607		-66323		-40409

Table 6. Calculation of internal rate of return for the recirculating system powered by photovoltaic solar system.

Year (m)	Cash flow (Naira) d_m	Trial for r = 0.1		Trial for r = 0.2		r = 0. 19	
		Factor	Present-worth (Naira)	Factor d_m	Present-worth (Naira)	Factor d_m	Present-worth (Naira)
0	(1059000)						
1	394400	0.909	358510	0.833	328535	0.840	331296
2	394400	0.826	325774	0.694	273714	0.705	278052
3	394400	0.751	296194	0.579	228358	0.592	233485
4	354400	0.683	242055	0.482	170821	0.497	176137
5	394400	0.621	244922	0.402	158549	0.417	164465
6	394400	0.564	222442	0.335	132124	0.350	138040
7	394400	0.513	202237	0.279	110038	0.294	115954
8	394400	0.466	183791	0.232	91501	0.247	97417
9	394400	0.424	167226	0.194	76514	0.207	81641
10	394400	0.385	151844	0.162	63893	0.174	68626
Total			2395085		1634047		1685113
Relationship = Total present-worth / Original investment			$\frac{2395085}{1059000}$ = 2.262		$\frac{1634047}{1059000}$ = = 1.543		$\frac{1685113}{1059000} = 1.591$
NPV			1336085		575047		626113

subtracting the costs from the revenue. The cash flow statement indicated the surplus (losses and /or gains) over the 10 year period. Also, the cash flow indicated how much of the loan could be repaid and during what period in the years of production. The balance sheet was used to keep track of the accounting of the farm. The profitability measurements showed how the cash flows could be used in the calculations of NPV and the IRR.

It should be noted that besides serving as a decision support tool for investment analysis, the profitability model can be used during operations as a planning tool year by year. The balance sheet reflected the assets and liabilities during the operations. Profitability measurements, IRR and financial ratios indicated the

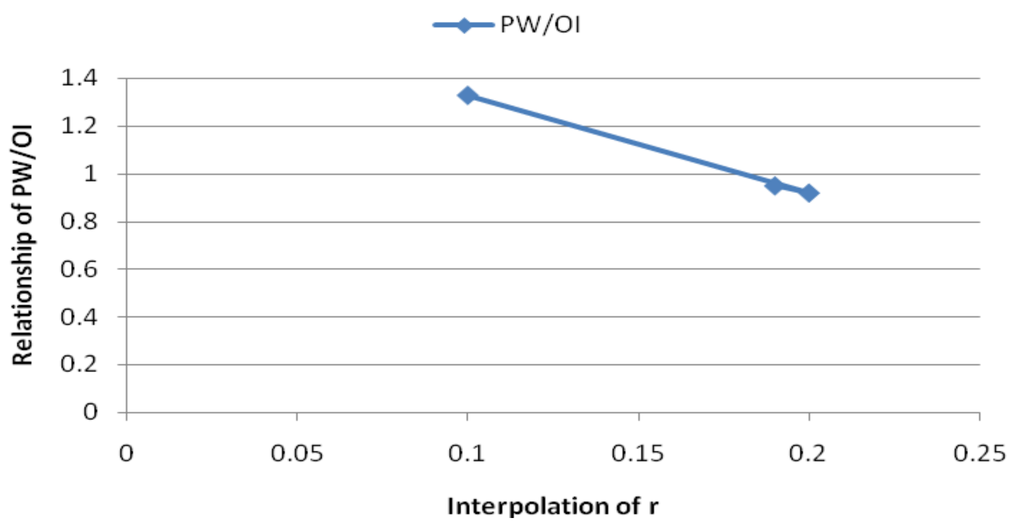

Figure 1. The relationship of PW/ O I and r in recirculating system powered with generator.

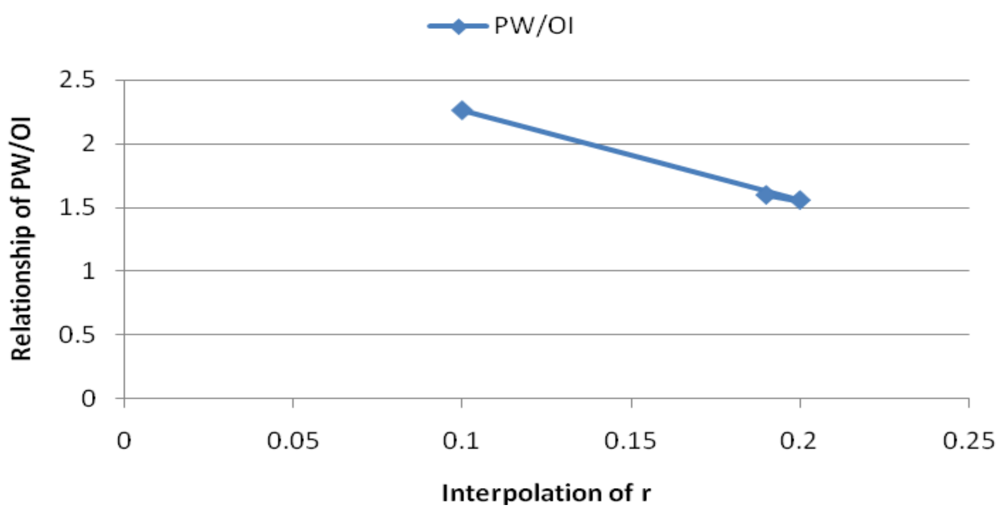

Figure 2. The relationship of PW / OI and r in recirculating system powered with photovoltaic.

feasibility of the venture over the years.

Pay time

Pay time for generator and solar photovoltaic were 4.53 and 2.69 years as calculated from the equation and can be determined by plotting the graph of accumulated cash against years (Tables 7 and 8). Tables 7 and 8 show accumulated cash flows for the recirculating system that was powered by generator and photovoltaic as power source. The cash flow accumulated, moving from negative to positive, and when the project ends, the capital invested in current assets and land would be recovered, resulting in a positive final cash flow. The cash flow was negative for 0 to 4th year for the recirculating system that was powered by generator and was only negative in 0-2nd year for the recirculating system that was powered by photovoltaic. This is an indication of the success of the venture since the accumulated cash flow was consistently positive after the 2nd year and 4th year in photovoltaic and generator system respectively.

DISCUSSIONS

To evaluate the profitability of the venture, indicators of investment returns were determined such as NPV, IRR and payback period (NAERL, 2000; Parin and Lupin,

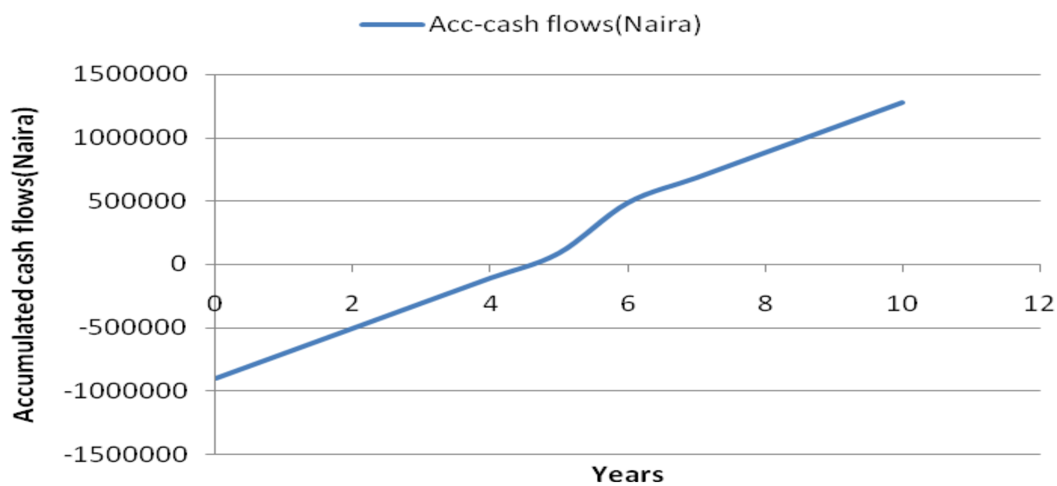

Figure 3. Accumulated Cash flow in generator powered recirculating system.

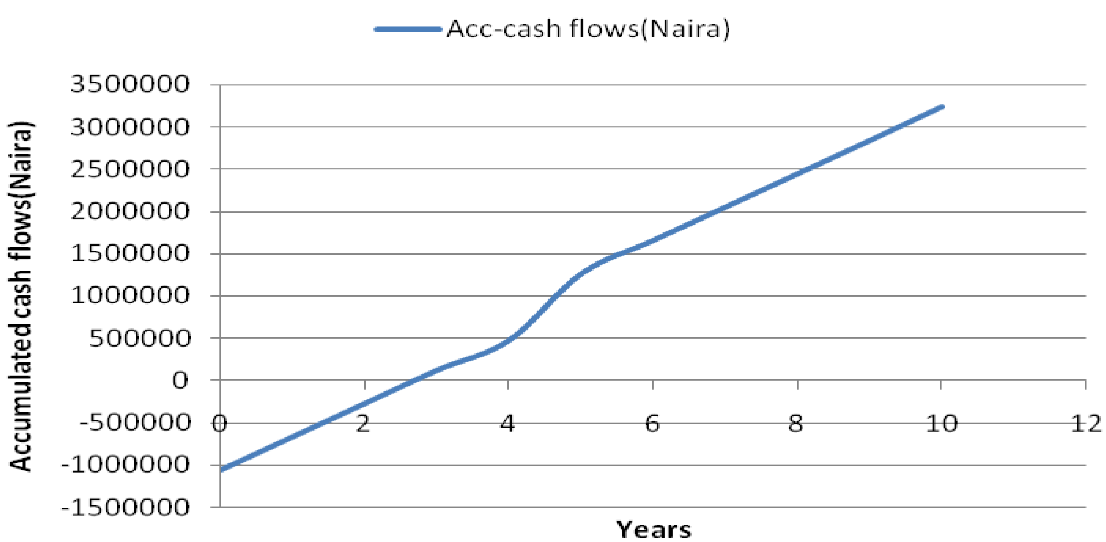

Figure 4. Accumulated Cash flow in recirculating system power with photovoltaic solar system.

Table 7. Accumulated cash flows for the recirculating system that uses generator as power source.

Years	Cash flow (Naira)	Accumulated cash flow (Naira)
0	-895500	-895500
1	197800	-697700
2	197800	-499900
3	197800	-302100
4	197800	-104300
5	197800	93500
6	197800	489100
7	197800	686900
8	197800	884700
9	197800	1082500
10	197800	1280300

Table 8. Accumulated cash flows for the recirculating system powered with photovoltaic.

Years	Cash flow (Naira)	Accumulated cash flow (Naira)
0	-1059000	-1059000
1	394400	-664600
2	394400	-270200
3	394400	124200
4	354400	478600
5	394400	1267400
6	394400	1661800
7	394400	2056200
8	394400	2450600
9	394400	2845000
10	399400	3244400

1995). The results obtained indicated positive NPV's in photovoltaic powered recirculating system and positive NPV in generator powered system where r = 0.1 while r = 0.2 and 0.19 recorded negative values of NPV. Key factors which affect profitability of operations in fish plants are generally cost and quality of raw material and the yield from processing, as long as the raw material is available and the market for the resulting products is stable (Parin and Lupin, 1995). The result of IRR and a payback period of 2.69 and 4.53 years obtained for photovoltaic and generator respectively were within the range that would be acceptable and profitable. Reduction in payback period is better in photovoltaic system because the project was able to recoup the original investment within a shorter period. Positive values of NPV as well as higher values of IRR in recirculating system powered with solar and reduced payback period are all indications that solar is a better option than generator despite its high initial capital investment. The methodology developed here can easily be adapted to evaluate any type of investment for instance fish farming enterprises of other species or fishery operations.

The challenge to designers of recirculating systems is to maximize production capacity of capital invested through employing the use of efficient energy sources to power the systems. Components should be designed and integrated into the complete system or existing fish ponds to reduce cost while maintaining or even improving reliability. There are many alternative technologies for each process and operation. The selection of a particular technology depends upon the species being reared, production site infrastructure, production management expertise, and other factors. Prospective users of recirculating aquaculture production systems need to know about the required water treatment processes, the components available for each process, and the technology behind each component. A recirculating system maintains an excellent cultural environment while providing adequate feed for optimal growth.

Conclusion

The result of IRR and a payback period of 2.69 and 4.53 years obtained for photovoltaic and generator, respectively were within the range that would be acceptable and profitable. Reduction in payback period is good because the project was able to recoup the original investment within a shorter period. Positive values of NPV as well as higher values of IRR in recirculating system powered with solar and reduced payback period are all indications that solar is a better option than generator despite its high initial capital. Further, it is anticipated that a successful and vibrant small scale recirculating system powered with solar could trigger a commercial recirculating system in the country. In addition, the small scale farmers might grow in capital and knowledge and transform themselves into medium and eventually large scale farmers.

REFERENCES

Duning RD, Losordo TM, Hobbs AO (1998). The Economics of Recirculating Tanks Systems, A Spreadsheet for Individual Analysis, Southern Regional Aquaculture Center, SRAC Publication No. 456.

Emperor Aquatics (2013). "Recirculating Systems in Aquculture". Available at http://www.emperoraquatics.com/aquaculture-recirculationsystems.php#.Um AMx6B59kg.

Food and Water Watch Report (2008). "Land Based Recirculating Aquacultural Systems". Available at www.foodandwaterwatch.org › Reports › Fish.

Losordo TM, Masser MP, Rakosy J (1998). Recirculating Aquaculture Tanks Production System, An Overview of Critical Considerations. Southern Regional Aquaculture Center, SRAC Publication No. 451.

Masser MP, Rakosy J, Losordo TM (1999). Recirculating Aquaculture Tanks Production System, Management of Recirculating System. Southern Regional Aquaculture Center, SRAC Publication No. 452.

NAERLS (2000). Econonomics of Aquacultural production. Extension Bulletin No107, Fisheries series No.5 published by National Agricultural Extension and Research Liaison services Ahmadu Bello University, Zaria.

Parin AZ, Lupin MH (1995). Food and Agriculture Organization of the United Nations. Fisheries Technical Paper, P. 351.

Poulson TM (2013). “Recirculating Aquaculture”. Available at http://www.eurofish.dk /~efweb/ images/stories/files/Turkey/8-TMP.pdf.

Rakacy JE (2006). “Recirculating Aquaculture Tank Production System”. Available at *www.ca.uky.edu/wkrec/454fs.PDF.*

Sioux Indian Reservation (2006). “Design Guide for Recirculating Aquaculture System”, Available at http://www.rowan.edu/colleges/engineering/clinics/engwoborders /Rep orts/EWB_fish_hatchery_final.pdf.

The Fish Site (2010). “Recirculating Water Systems used for Fish Production”, Available at http://www.thefishsite.com/fishnews/13400/recirculating-water-systems-used-for-fish-production.

Zhang SY, Gu L, Hui BW, Xing GL, Yan HY, Ling T, Hung L (2011). “An Integrated RecirculatingAquaculture System for Land-Based Fish Farming. The Effects of Water Quality and Fish Production. Aquacultural Eng. 45(3):93-102.

academicJournals

Vol. 8(43), pp. 2011-2022, 23 November, 2013
DOI: 10.5897/IJPS2013.4051
ISSN 1992 - 1950 © 2013 Academic Journals
http://www.academicjournals.org/IJPS

International Journal of Physical Sciences

Full Length Research Paper

Optimization of the louver angle and louver pitch for a louver finned and tube heat exchanger

Jiin-Yuh Jang* and Chun-Chung Chen

Department of Mechanical Engineering, National Cheng Kung University, Tainan 70101, Taiwan.

Accepted 14 November, 2013

The optimization of the louver angle (θ) and the louver pitch (Lp) for a louver finned and tube heat exchanger was investigated numerically along with a simplified conjugate-gradient method (SCGM). The area reduction ratio relative to a plain surface is the objective function to be maximized. A search for the optimum louver angle (θ) and louver pitch (Lp), ranging from 15°< θ < 40° and 2 mm < Lp < 3.2 mm, respectively, was performed. The results showed that the maximum area reduction ratios may reach 39~46% combined with the optimal design of (θ, Lp) at Re_D = 589~3533 (U_{in}= 0.5-3.0 m/s).

Key words: Optimization, louver pitch, louver angle, finned and tube heat exchanger.

INTRODUCTION

Fin-and-tube heat exchangers with louvered fins are widely employed in automobiles, air-conditioners and power generation, etc. The louvers act to interrupt the airflow and create a series of thin boundary layers that have lower thermal resistance. The first reliable published data on louvered fin surfaces was presented by Kays and London (1950). Davenport (1983) utilized smoke trace to study a standard variant of the corrugated louvered fin geometry and obtained heat transfer and friction correlations for corrugated louvered fin geometry. Achaichia and Cowell (1988) made an overall study of performance characteristics of flat-sided tube and louvered plate fin heat exchangers. They obtained the correlations for the louvered plate fin geometry. Sahnoun and Webb (1992) developed an analytical model to predict the heat transfer and friction characteristics of the corrugated louvered fin core. Sunden and Svantesson (1992) presented the investigations of heat transfer and pressure drop of standard louver fin and inclined louver fin. Their investigations illustrate that all the louvered surfaces are better efficient than the corresponding smooth surface. Wang et al. (1998) tested 17 samples of commercially available louver fin and tube heat exchangers for different geometrical parameters, including the number of tube row, fin pitch, and tube size.

In the 1990’s, some investigators developed CFD code based on non-orthogonal, boundary-fitted meshes to calculate the flow over louvered fins. Suga et al. (1990) and Suga and Aoki (1991) used a rectangular flow domain filled with overlapping Cartesian meshes to calculate the flow and heat transfer over a finite-thickness fin. Hiramatsu et al. (1990) and Ikuta et al. (1990) utilized a block structured mesh with respective blocks for each louver.

Jang et al. (2001) numerically researched a three dimensional convex louver finned tube heat exchangers. The effects of different geometrical factor, containing convex louver angles (15.5°, 20.0°, 24.0°), louver pitch (0.953 mm, 1.588 mm) and fin pitch (8 fins/in., 10 fins/in., 15 fins/in.) are studied in detail for the Reynolds number ranging from 100 to 1100. It was proven that, for equal louver pitch, both the average Nusselt number and pressure drop coefficient are increased as the louver angle is increased; while for equal louver angles, they are

*Corresponding author. E-mail: jangjim@mail.ncku.edu.tw, Tel: +886-6-2757575 ext. 62148, Fax: +886-6-2088573.

decreased as the louver pitch is increased. Hsieh and Jang (2006) proposed continuously increased or decreased louver angle models and carried out a 3-D numerical analysis on heat transfer and fluid flow. Their results showed that continuously variable louver angle types employed in heat exchangers could effectively enhance the heat transfer performance. They also revealed that the maximum area reduction could reach up to 25.5% compared with a plain fin surface. Jang and Tsai (2011) utilized the simplified conjugate-gradient method (SCGM) to search the optimal louver angle of a fin heat exchanger. The area reduction for using louver surface compared to the plain surface was the objective function to be maximized. The maximum area reduction ratios of the louvered fins were 65.3, 66.9, 65.6, 63.7 and 62.2% with Re = 100 ~ 500 and Lp = 1.0 mm. Hsieh and Jang (2012) numerically studied the optimal design of a louver finned-tube heat exchanger applying the Taguchi method. Eighteen kinds of patterns were made by mixed levels on each factor. The optimal design values for each parameter were all reported.

The foregoing literature review reveals that no related 3-D numerical analysis for the optimization of louvered angle and louvered pitch and their coupled effects on the thermal and hydraulic characteristics of a louver finned and tube heat exchanger has been published. This has motivated the present investigation. In the present research, the optimization of louver angle and its pitch is studied and solved numerically using a commercial CFD code ANSYS FLUENT (2009) along with a simplified conjugate-gradient method. To achieve optimization goals, the area reduction ratio is the objective function to be maximized. The influence of louver pitch (Lp = 2.0 ~ 3.2 mm) and louver angle (θ = 15°< θ < 40°) on the heat transfer performance and friction loss at different Reynolds numbers are discussed in detail. The optimal design values for two operating parameters at different Reynolds number are also presented.

MATHEMATICAL ANALYSIS

Governing equation

Figure 1 describes the physical model and relevant geometric dimensions of the louver finned and tube heat exchanger. The unit is a mini-meter. The louver angle (θ = 15° ~ 40°) and louver pitch (Lp = 2.0 ~ 3.2 mm) as shown in Figure 2 are the main operating parameters in the present study. The fluid is considered 3-D incompressible turbullent flow with constant properties, and the flow is assumed to be steady with no viscous dissipation. Equations for continuity, momentum (Reynolds averaged Navier-Stokes equations), energy, turbulent kinetic energy, k, and the dissipation rate, ε, can be expressed in tensor form as follows:

$$\frac{\partial \overline{u_i}}{\partial x_i} = 0 \tag{1}$$

$$\frac{\partial}{\partial x_j}\rho\left(\overline{u_i u_j}\right) = -\frac{\partial \overline{P}}{\partial x_i} + \frac{\partial}{\partial x_j}\left[\mu_{eff}\left(\frac{\partial \overline{u_i}}{\partial x_j} + \frac{\partial \overline{u_j}}{\partial x_i}\right) - \rho\left(\overline{u_i' u_j'}\right)\right] \tag{2}$$

$$\frac{\partial}{\partial x_j}\rho C\left(\overline{u_j T}\right) = \overline{u_j}\frac{\partial \overline{P}}{\partial x_j} + \overline{u_j'}\frac{\partial \overline{P'}}{\partial x_j} + \frac{\partial}{\partial x_j}\left[k\frac{\partial \overline{T}}{\partial x_j} - \rho C\overline{u_j' T'}\right] \tag{3}$$

$$\frac{\partial}{\partial x_i}\left(\rho \overline{u_i} k\right) = -\frac{\partial}{\partial x_i}\left(\frac{\mu_{eff}}{\sigma_k}\frac{\partial k}{\partial x_i}\right) + \rho(\Pr - \varepsilon) \tag{4}$$

$$\frac{\partial}{\partial x_i}\left(\rho \overline{u_i}\varepsilon\right) = -\frac{\partial}{\partial x_i}\left(\frac{\mu_{eff}}{\sigma_\varepsilon}\frac{\partial \varepsilon}{\partial x_i}\right) + \rho\frac{\varepsilon}{k}\left[\left(c_1 + c_3\frac{\Pr}{\varepsilon}\right)\Pr - c_2\varepsilon\right] \tag{5}$$

where $\Pr = (\mu_t/\rho)[2(\partial u_i/\partial x_i)^2 - 2(\nabla u_i)^2/3]$, $\mu_{eff} = \mu + \mu_t$, $\mu_t = \rho c_\mu\left(k^2/\varepsilon\right)$, $c_\mu = 0.09$, $c_1 = 0.15$, $c_2 = 1.90$, $c_3 = 0.25$, $\sigma_k = 0.75$ *and* $\sigma_\varepsilon = 1.15$

Equation 2 contains Reynolds stresses that are modeled by Chen's extended k-ε turbulence model (Chen and Kim, 1987; Wang and Chen, 1993), where k is the turbulent kinetic energy, and ε is the dissipation rate. In Chen's model, the production time scale as well as the dissipation time scale is used in closing the ε equation. This extra production time scale is claimed to allow the energy transfer mechanism of turbulence to respond to the mean strain rate more effectively. This results in an extra constant in the ε equation. As to the velocity distribution in the near-wall region ($y^+ \leq 11.63$), the following law of the wall (Liakopoulos, 1984) is applied:

$$u^+ = \ln\left[\frac{(y^+ + 11)^{4.02}}{({y^+}^2 - 7.37y^+ + 83.3)^{0.79}}\right] + 5.63\tan^{-1}(0.12y^+ - 0.441) - 3.81 \tag{6}$$

Where

$$y^+ \equiv \frac{\rho u_\tau y}{\mu} \text{ and } u_\tau = \sqrt{\frac{\tau_w}{\rho}} \tag{7}$$

Parameter definition of performance factor

The local pressure drop can be expressed in terms of the dimensionless pressure coefficient C_p defined as:

$$Cp = \frac{p - p_{in}}{\frac{1}{2}\rho {U_{in}}^2} \tag{8}$$

where P_{in} is the pressure at inlet and U_{in} is the inlet velocity. The local heat transfer coefficient *h* is defined as:

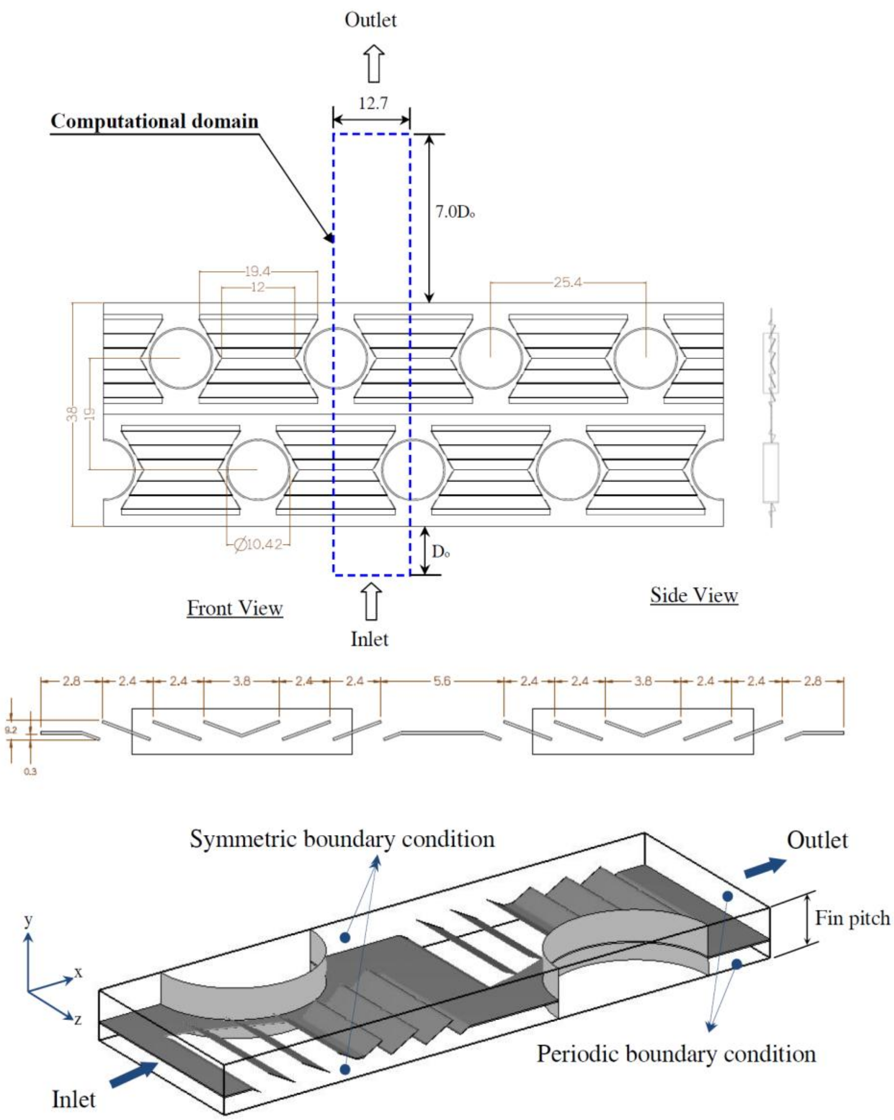

Figure 1. The physical model and computational domain (fin thickness, t =0.115 mm).

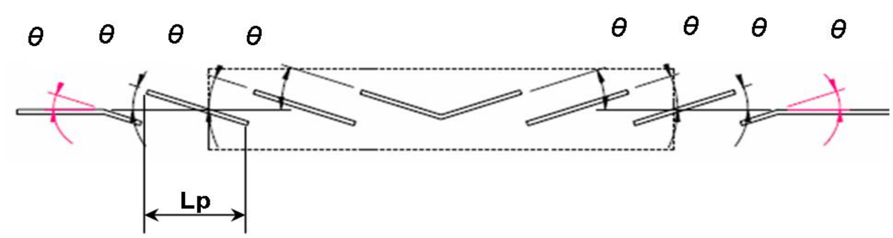

Louver angle θ	15°	20°	25°	30°	35°	40°	
Louver pitch Lp	2.0mm	2.2mm	2.4mm	2.6mm	2.8mm	3.0mm	3.2mm

Figure 2. The louver pattern for different louver angles and louver pitches.

$$h = \frac{q''}{T_w - T_b} \tag{9}$$

where q'' is the local heat flux. T_b is the local bulk mean temperature. T_w is the wall temperature. The local heat transfer coefficient can be expressed in the dimensionless form by the Nusselt number *Nu*, defined as:

$$Nu = \frac{h \cdot D_o}{k} = \frac{\partial \left[\frac{\Theta}{\Theta_b} \right]_{wall} \cdot D_o}{\partial \mathrm{n}} \tag{10}$$

where $\Theta_b = (T_b - T_{in})/(T_w - T_{in})$ is the local dimensionless bulk mean temperature and *n* is the dimensionless unit vector normal to the wall and D_o is the outside diameter of tube. The average Nusselt number $\overline{Nu}$ can be obtained by

$$\overline{\mathrm{Nu}} = \frac{\int \mathrm{Nu}\, \mathrm{dA_s}}{\int \mathrm{dA_s}} \tag{11}$$

where dA_s is the infinitesimal area of the wall surface. The friction factor f and Colburn factor j are defined as:

$$f = \frac{p - p_{in}}{\frac{1}{2}\rho U_{in}^{\ 2}} \times \frac{D_o}{4L} \tag{12}$$

$$j = \frac{\overline{\mathrm{Nu}}}{\mathrm{Re}_D \mathrm{Pr}^{1/3}} \tag{13}$$

where P_{in} is the pressure at the inlet, L is the flow length, Re_D is the Reynolds number defined as $\mathrm{Re}_D = \mathrm{U_{max}} \mathrm{D_o}/\nu$, U_{max} is the air velocity at minimum free flow area, Pr is the Prandtal number defined as $\mathrm{Pr} = \nu/\alpha$, α is the thermal diffusivity, and ν is the kinematic viscosity.

Boundary condition

Since the governing equations are elliptic, it is necessary to impose boundary conditions at all of the boundaries in the computational domain. The upstream boundary is established at a distance of one tube diameter in front of the leading edge of the fin. At this boundary, the flow velocity U_{in} is assumed to be uniform, and the temperature T_{in} is taken to be 300K. At the downstream end of the computational domain, located seven times the tube diameter from the last downstream row tube, the streamwise gradients (Neumann boundary conditions) for all the variables are set to zero. At the solid surfaces, no-slip conditions and constant wall temperature T_W (353K) are specified. On the symmetry planes (two X-Y planes), normal gradients are set to zero. On the upper and lower X-Z planes, periodic boundary conditions are imposed. Additionally, at the solid-fluid interface,

$$\mathrm{T_s} = T_f \ ; \ -k_s \cdot \partial T_s / \partial n = -k_f \cdot \partial T_f / \partial n \tag{14}$$

Performance evaluation criteria (PEC)

Many performance evaluation criteria (PEC) have been developed for evaluating the performance of heat exchangers. The VG-1 (variable geometry) performance criteria, as described by Webb (1994), represents the possibility of surface area reduction by using enhanced surfaces having fixed heat duty, temperature difference and pumping power.

$$\frac{hA}{h_o A_o} = \frac{j}{j_o} \frac{A}{A_o} \frac{G}{G_o} \tag{15}$$

where the subscripts of 'o' refer to the reference plate fin, and *G* is the mass velocity. The pumping power is calculated as:

$$\omega = \left(f \frac{A}{A_m} \frac{G^2}{2\rho} \right) \left(\frac{G A_m}{\rho} \right) \tag{16}$$

where A_m is the flow area at minimum cross section. The pumping power ratio relative to the reference plane fin can be obtained by:

$$\frac{\omega}{\omega_o} = \frac{f}{f_o} \frac{A}{A_o} \left(\frac{G}{G_o} \right)^3 \tag{17}$$

and by the elimination of the term

$$\frac{hA / h_o A_o}{(\omega / \omega_o)^{1/3} (A / A_o)^{2/3}} = \frac{j / j_o}{(f / f_o)^{1/3}} \tag{18}$$

Under the pumping power constraint of case VG-1, that is ($\omega/\omega_o = 1$), we may obtain the area reduction ratio relative to the reference plane fin as:

$$\frac{A}{A_o} = \left(\frac{f}{f_o} \right)^{1/2} \left(\frac{j_o}{j} \right)^{3/2} \tag{19}$$

NUMERICAL METHOD AND OPTIMIZATION

In this study, the governing equations are solved numerically using a control volume based finite difference formulation, ANSYS FLUENT

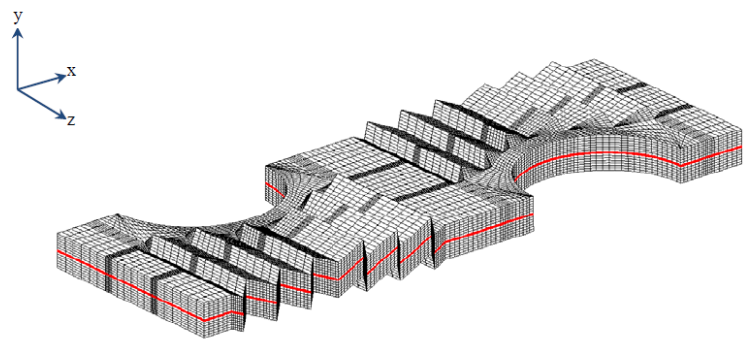

Figure 3. Computational grid system.

(2009). The numerical methodology is briefly described here. Finite difference approximations are employed to discretize the transport equations on non-staggered grid mesh systems. A third-order upwind TVD (total variation diminishing) scheme is used to model the convective terms of governing equations. Second-order central difference schemes are used for the viscous and source terms. A pressure based predictor/multi-corrector solution procedure is employed to enhance velocity–pressure coupling and continuity-satisfied flow filed. A grid system of 288 × 19 × 31 grid points was adopted typically in the computation domain as shown in Figure 3. However, a careful check for the grid-independence of the numerical solutions has been made to ensure the accuracy and validity of the numerical results. For this purpose, three grid systems, 335 × 23 × 37, 288 × 19 × 31 and 241 × 14 × 23, were tested. It was found that for U_{in} = 3.0 m/s, the relative errors in the local pressure and temperature between the solutions of 335 × 23 × 37, 288 × 19 × 31 were less than 3%. The convergence criterion is satisfied when the residuals of all variables are less than 1.0×10^{-7}. Computations were performed on a Pentium 4 3.0G personal computer and typical CPU times were 5000–6000 s.

In the present study, the simplified conjugate-gradient method (Jang and Tsai, 2011) is combined with a finite differential method code (ANSYS FLUENT, 2009) as an optimizer to search the optimum louver angle (θ) and louver pitch (Lp). The objective functions $J\ (x_1,x_2)$ are defined as the maximum area reduction ratio relative to the palin fin surface (1-A/A_o).

Above all, the SCGM method evaluates the gradient of the objective function, and then it sets up a new conjugate direction for the updated design variables with the help of a direct numerical sensitivity analysis. The initial guess for the value of each search variable is made, and in the successive steps, the conjugate-gradient coefficients and the search directions are evaluated to estimate the new search variables. The solutions obtained from the finite difference method are then used to calculate the value of the objective function, which is further transmitted back to the optimizer for the purpose of calculating the consecutive searching directions. The procedure for applying this method is described in the following:

(1) Generate an initial guess for two design variables (x_1,x_2) –louver angle (θ) and and louver pitch (Lp).
(2) Adopt the finite difference method to predict the velocity field (U) and temperature fields (T) associated with the latest θ and Lp, and then calculate the objective function $J\ (x_1,x_2)$.
(3) When the value of $J(x_1,x_2)$ reaches a maximum, the optimization process is terminated. Otherwise, proceed to step 4.
(4) Determine the gradient functions, $(\partial J/\partial x_1)^{(k)}$ and $(\partial J/\partial x_2)^{(k)}$, by applying a small perturbation ($\Delta x_1,\Delta x_2$) to each value of x_1 and x_2, and calculate the corresponding change in objective function (ΔJ). Then, the gradient function with respect to each value of the design variables (x_1,x_2) can be calculated by the direct numerical differentiation as

$$\frac{\partial J_1^{(k)}}{\partial x_1} = \frac{J_1^{(k)} - J^{(k)}}{\Delta x_1} \text{ and } \frac{\partial J_2^{(k)}}{\partial x_2} = \frac{J_2^{(k)} - J^{(k)}}{\Delta x_2} \tag{20}$$

(5) Calculate the conjugate-gradient coefficients $\gamma^{(k)}$, and the search directions, $\xi_1^{(k+1)}$ and $\xi_2^{(k+1)}$, for each search variable. For the first step with k = 1, $\gamma^{(1)} = 0$.

$$\gamma^{(k)} = \frac{\sum_{n=1}^{2}\left(\frac{\partial J_n^{(k)}}{\partial x_n}\right)^2}{\sum_{n=1}^{2}\left(\frac{\partial J_n^{(k-1)}}{\partial x_n}\right)^2} \tag{21}$$

$$\xi_1^{(k)} = \frac{\partial J_1^{(k)}}{\partial x_1} + \gamma^{(k)}\xi_1^{(k-1)} \text{ and } \xi_2^{(k)} = \frac{\partial J_2^{(k)}}{\partial x_2} + \gamma^{(k)}\xi_2^{(k-1)} \tag{22}$$

(6) Assign values to the coefficients of descent direction (β) for all values of the design variables (x_1, x_2). Specifically, those values are chosen by a trial-and-error process. In general, the coefficients of descent direction (β) are within a range of 0.2 ~ 0.01.
(7) Update the design variables with

$$x_1^{(k+1)} = x_1^{(k)} + \beta\xi_1^{(k)} \text{ and } x_2^{(k+1)} = x_2^{(k)} + \beta\xi_2^{(k)} \tag{23}$$

A flowchart of the SCGM optimization process is plotted in Figure 4.

RESULTS AND DISCUSSION

The present study mainly evaluated the influences of louver angle (θ) and louver pitch (Lp) on the local and overall flow and heat transfer characteristics of louver finned and tube heat exchangers. Furthermore, optimization analyses to θ and Lp were utilized in order to search the optimum combination of (θ, Lp) and maximum objective function (1 – A/A_0). The relevant numerical results were achieved in the range of 589 < Re_D < 3533 (0.5m/s < U_{in} < 3.0m/s), 15° < θ < 40°, and 2.0 mm < Lp < 3.2 mm. In order to validate the reliability of the numerical

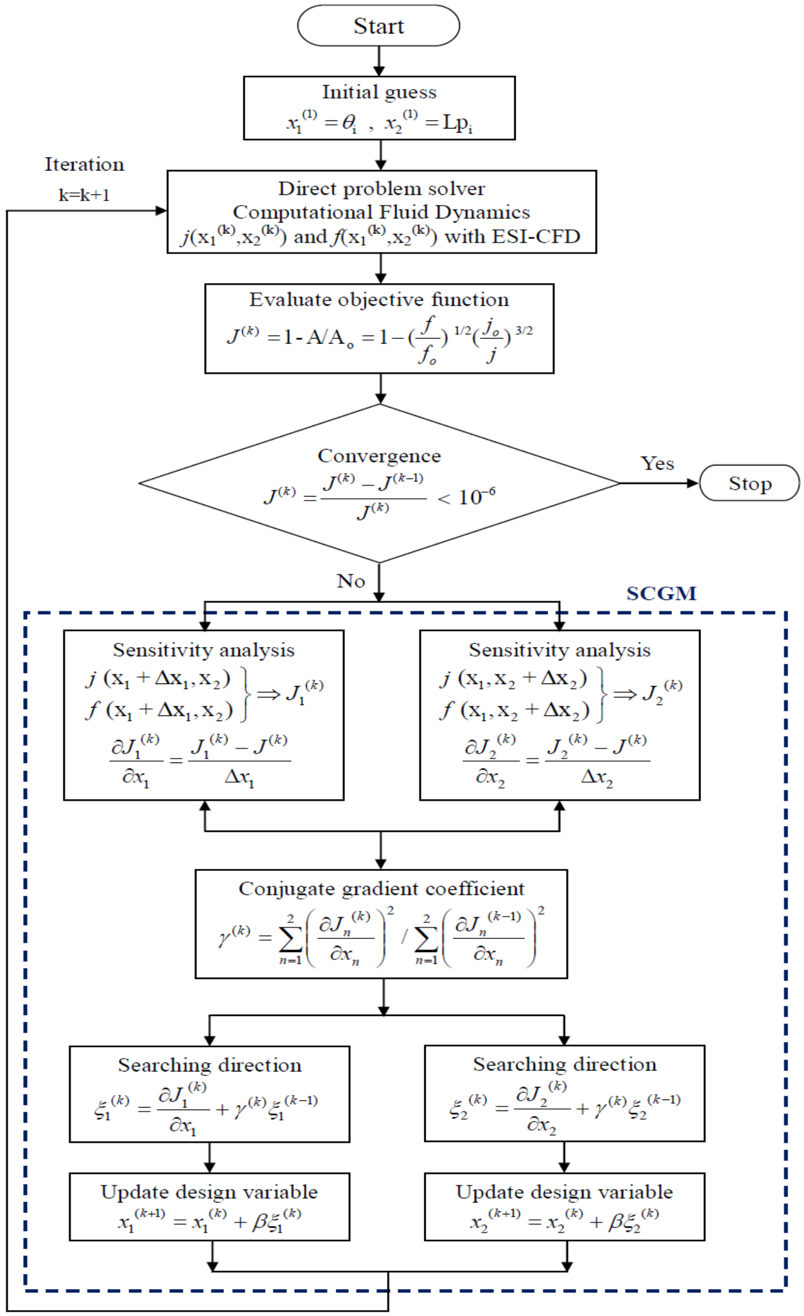

Figure 4. Flowchart for the optimization method.

simulation procedure, numerical simulations were carried out at the same operating conditions as the experimental louver finned-tube heat exchangers with two rows (Wang et al., 1998). Figure 5 shows the comparisons of j and f factors between the simulated results and the experimental results. The present results showed good agreements within a maximum of 10% discrepancy.

The flow and thermal field of a louver finned and tube heat exchanger is very complicated. Figure 6a and b show the streamline velocity and temperature distribution, respectively, for louver finned-tube with U_{in} =3.0 m/s, θ=15° and Lp=2.4 mm. The flow entering a louvered fin array quickly becomes louver directed. Then the flow passing the round cylinder (the first row of tubes) divides into opposite paths of equal velocity and path length over the cylinder surface. Apparently, the streamlines near the tube side wall are very dense and flow velocity accelerates quickly. The reason is that, the geometric shape of the channel near the tube side wall is convergent and divergent. The vortices appear at the downstream behind

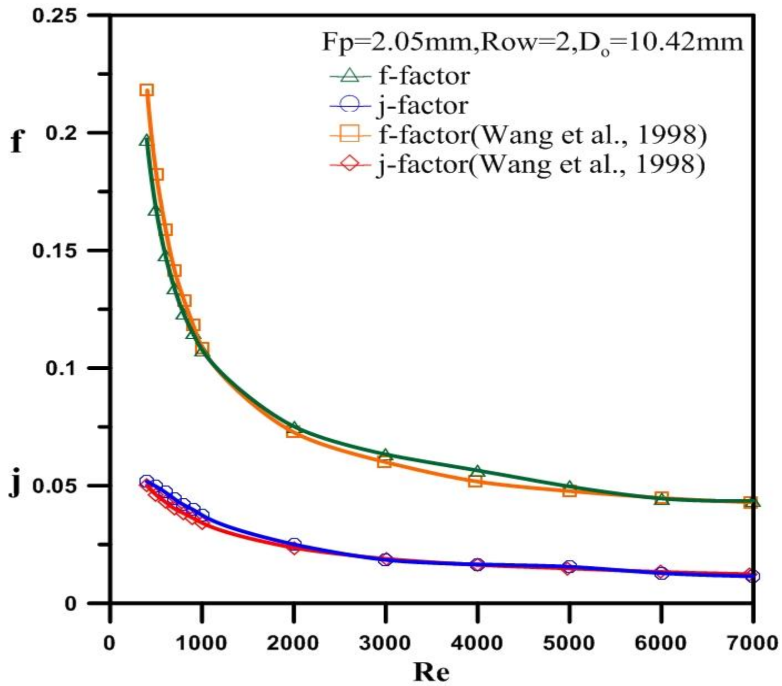

Figure 5. Comparison of the j and f factors for the present study and previous literature.

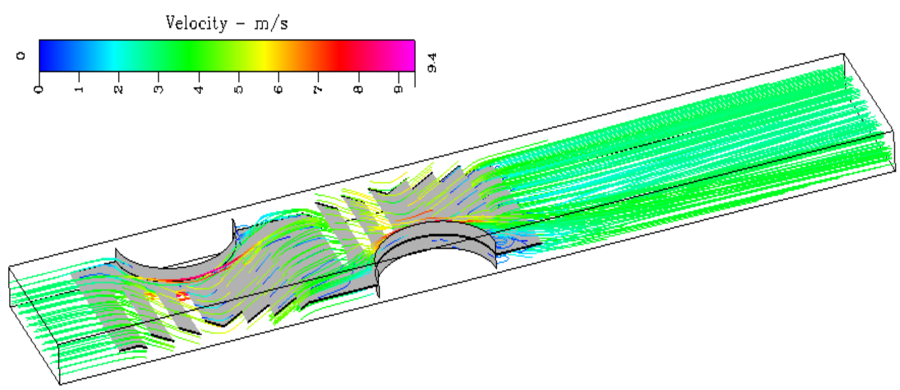

(a)

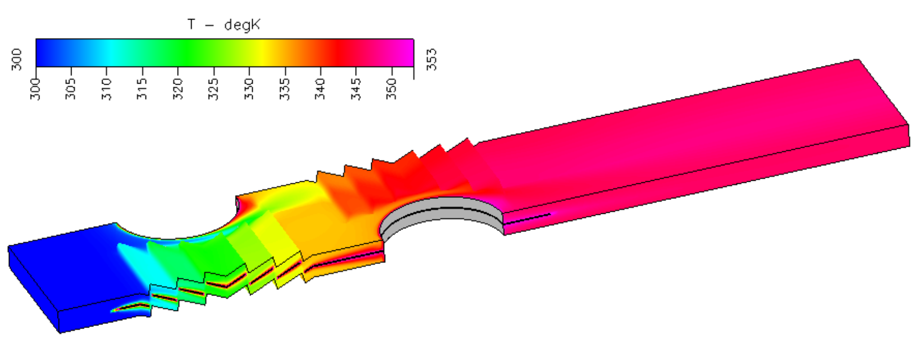

(b)

Figure 6. (a) Streamline velocity and (b) temperature distribution with Re=3533(U_{in}=3.0m/s) for θ = 15° and Lp=2.4 mm.

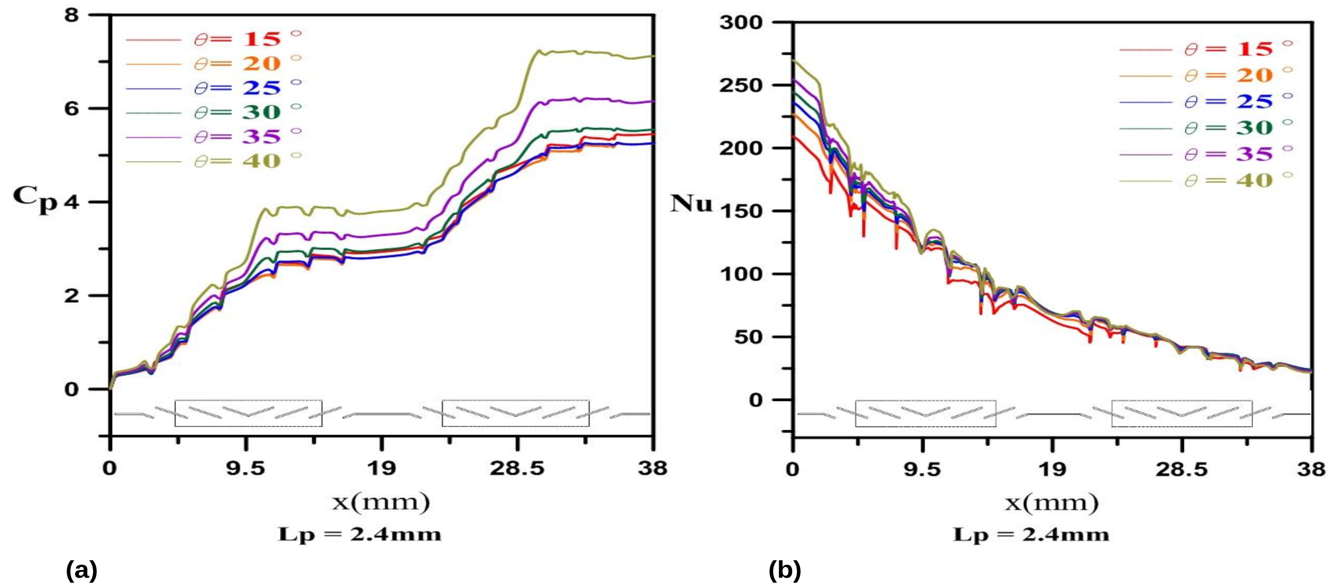

Figure 7. The variation of (a) C_p and (b) Nu along downstream direction for different louver angle with Re=3533(U_{in}=3.0m/s).

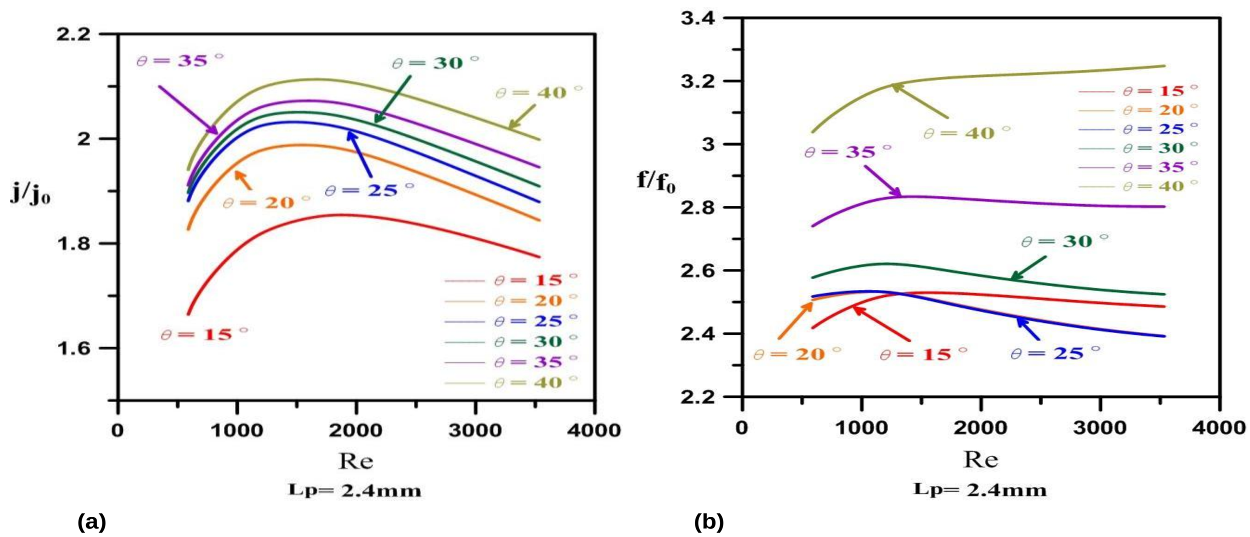

Figure 8. The (a) j/j_o and (b) f/f_o versus Reynolds number for different louver angle (θ) with louver pitch (Lp=2.4 mm).

the tube cylinder. The temperature gradients near the wall are quite large, which indicates a corresponding enhanced heat transfer.

Figure 7a and b present the variations of the local pressure drop coefficient (C_p) and Nusselt number (Nu), respectively, along the downstream direction with inlet frontal velocity (U_{in} = 3.0 m/s) and louver pitch (Lp =2.4 mm) for six different louver angles (θ = 15, 20, 25, 30, 35 and 40°). One can see that the there is a local maximum of Nu at the upstream inlet.

To evaluate how much performance is improved, j/j_o and f/f_o are used to interpret the data, where j/j_o and f/f_0 are the Colburn factor ratio and friction factor ratio between louver and without louver, respectively. Figures 8a and b illustrate the variations of j/j_o and f/f_o, versus Re_D, respectively, for six different louver angles (15, 20, 25, 30, 35 and 40°) with louver pitch (Lp=2.4 mm). The maximum heat transfer improvement interpreted by j/j_o are 1.853, 1.985, 2.026, 2.047, 2.071 and 2.113, and the corresponding friction factor ratio f/f_o are 2.528, 2.494, 2.492, 2.597, 2.829 and 3.211, respectively.

Figure 9a and b illustrate the variations of j/j_o and f/f_o versus Re, respectively, for seven different louver pitch (2.0, 2.2, 2.4, 2.6, 2.8, 3.0, and 3.2 mm) with louver angle

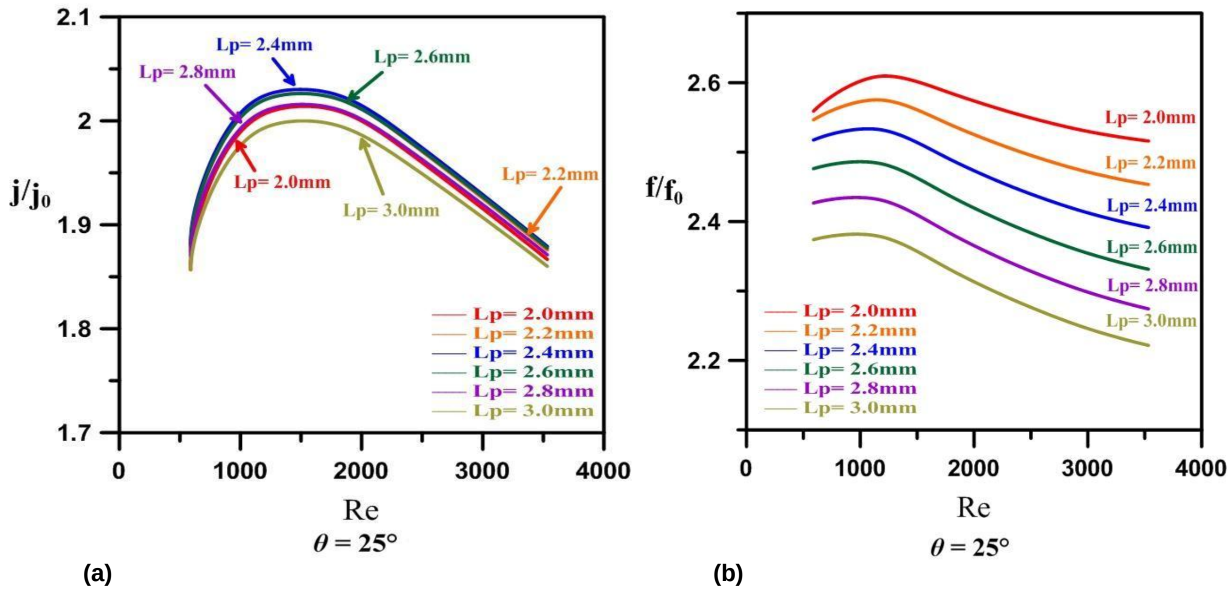

Figure 9. The (a) j/j_o and (b) f/f_o Reynolds number for different louver pitch (Lp) with louver angle (θ=25°).

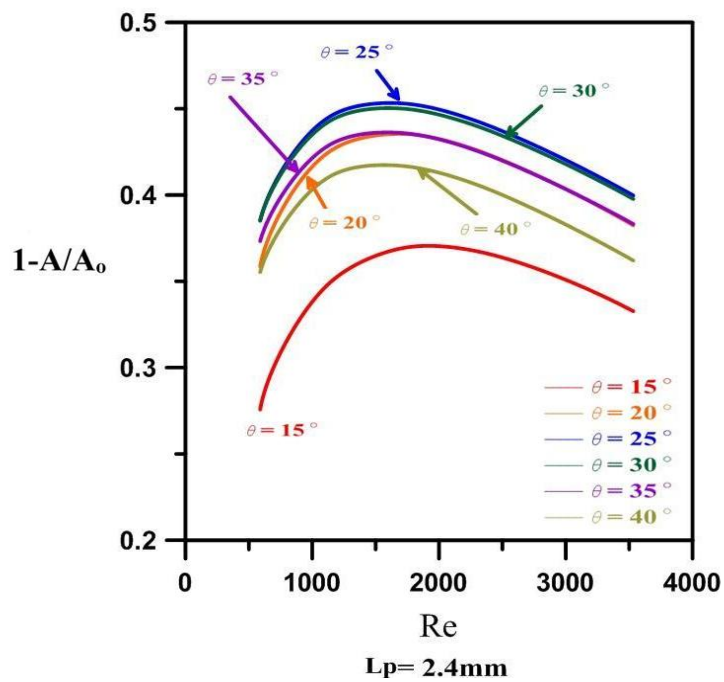

Figure 10. The area reduction versus Reynolds number for different louver angle (θ) with louver pitch (Lp=2.4 mm).

(θ=25°). The maximum heat transfer improvement interpreted by j/j_o are 2.011, 2.023, 2.026, 2.022, 2.012, 1.997 and 1.976, and the corresponding friction factor ratio f/f_o are 2.587, 2.541, 2.492, 2.439, 2.385, 2.333 and 2.286, respectively. The present results indicated that the variable louver angle and pitch patterns applied in heat exchangers could effectively enhance the heat transfer performance.

The possible area reduction $1\text{-}A/A_o$ (where A and A_o denote the surface areas for variable louver θ ranging from 15 to 40° and conventional plain fins, respectively) with Lp = 2.4 mm is presented in Figure 10. One can see

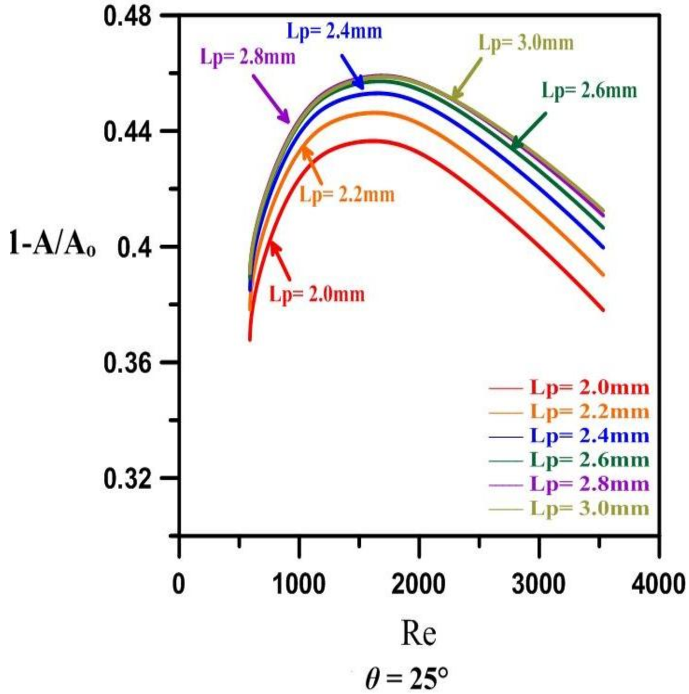

Figure 11. The area reduction versus Reynolds number for different louver pitch (Lp) with louver angle (θ=25°).

that the greatest area reduction ratio is as much as 37.0, 43.5, 45.3, 45.0, 43.5 and 41.6% with specific values of Re_D = 589, 1178, 1766, 2355, 2944 and 3533, respectively, it gives the greatest area reduction at Re = 1766 and θ =25°. Figure 11 presents the area reduction ratio for Lp ranging from 2.0 to 3.2 mm with θ = 25°, the greatest area reduction ratio is as much as 43.6, 44.6, 45.3, 45.7, 45.9, 45.9 and 45.6% with specific values of Re = 589, 1178, 1766, 2355, 2944 and 3533, respectively, it gives the greatest area reduction at Re = 1766 and Lp=3.0 mm.

Figure 12 displays the iteration process used to search the optimum louver angle (θ) and louver pitch (Lp) combination for the maximization of objective function (that is, area reduction ratio, $1\text{-}A/A_o$) at Re_D = 1766 (U_{in} = 1.5 m/s). The constant area reduction ratio contours are plotted as a function of θ and Lp, where the dark red area represents the maximum area reduction ratio. It is seen that, with the initial values (θi = 15° ,Lpi = 3.0 mm) and (θi = 40°, Lpi = 3.0 mm), by using the simple conjugated gradient method (SCGM), the optimal θ and Lp combination is obtained (θ = 24.09°, Lp = 2.91 mm) for around 19 and 18 iterations, respectively. The area reduction ratio is 45.9%. Thus, the current optimization method provides a tremendous savings in regard to computational time for the present physcial model. The searched optimum combination of θ and Lp with specific values of Re_D = 589, 1178, 1766, 2355, 2944 and 3533 (U_{in}=0.5 to 3.0 m/s) are tabulated in Table 1. It is seen that, an area reduction ratio of 39 to 46% is achieved across the range of Re_D.

Conclusion

Three dimenional turbulent fluid flow and heat transfer in two row fin-and-tube heat exchanger with and without louver fins are studied numerically. The optimization of the louvered angle (θ) and louvered pitch (Lp) is executed by using a simplified conjugate-gradient method. A searched procedure for the optimum louver angle (θ) and louver pitch (Lp), ranging from 15°< θ < 40° and 2.0 mm < Lp < 3.2 mm, respectively, is executed. The searched optimum objective function associated with an optimal combination of θ and Lp for different Re_D are obtained for less than 30 iterations. This demonstrates that the current optimization method provides a tremendous savings in regard to computational time for the present physcial model. In addition, the results showed that the maximum area reduction ratios may reach 39~46% combined with the optimal design of (θ, Lp) at U_{in}= 0.5~3.0 m/s.

ACKNOWLEDGEMENT

Financial support for this work was provided by the National Science Council of Taiwan, under contract NSC NSC 101-2221-E-006 -109 -MY2.

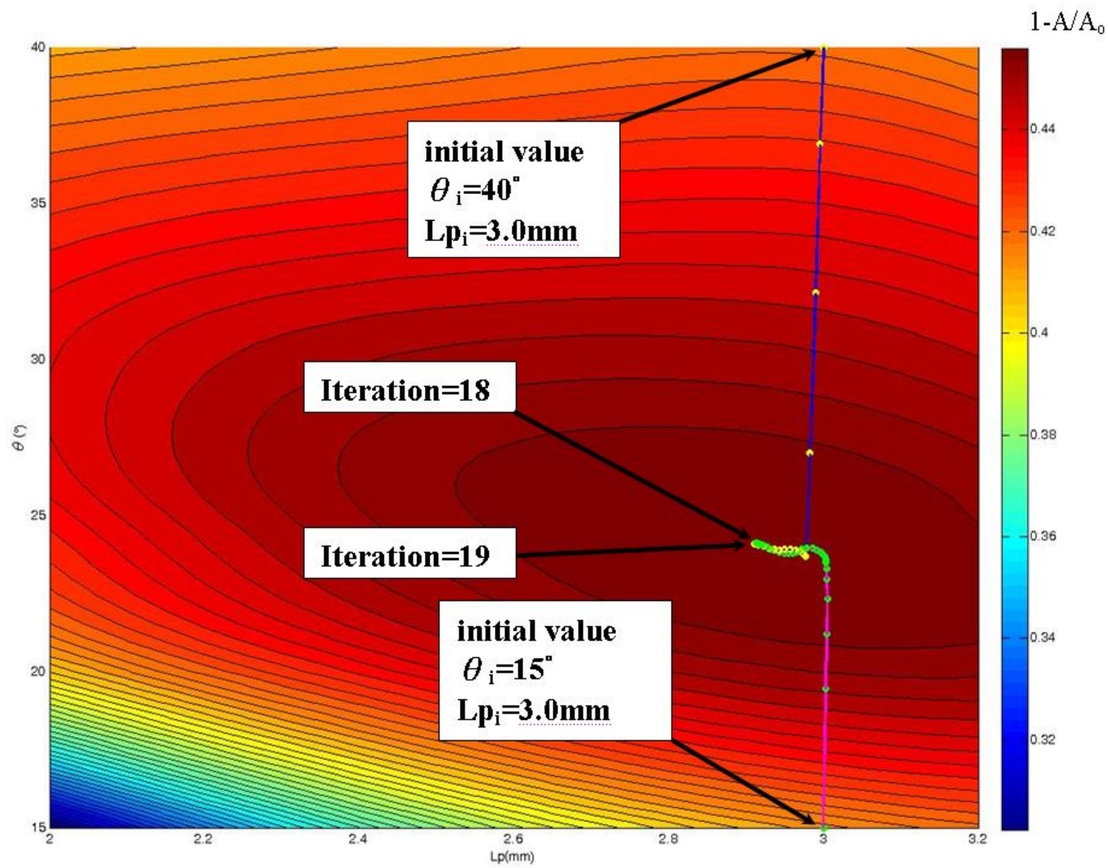

Figure 12. Iteration process to search the optimum combination of θ and Lp (U_{in}=1.5m/s).

Table 1. The searched optimum combination of θ and Lp for different Re_D.

Re	U_{in}(m/s)	Initial value		θ	Lp(mm)	j/j_o	f/f_o	$1-A/A_o$ (%)	Iteration numbers
		$θ_i$	Lp_i						
589	0.5	15.0	3.0	25.11	2.93	1.862	2.393	39.1	29
1178	1.0	15.0	3.0	24.23	2.88	2.003	2.411	45.2	25
1766	1.5	15.0	3.0	24.09	2.91	2.004	2.353	45.9	19
2355	2.0	15.0	3.0	24.10	2.97	1.963	2.291	45.0	18
2944	2.5	15.0	3.0	24.47	2.98	1.912	2.251	43.3	13
3533	3.0	15.0	3.0	24.80	2.99	1.859	2.220	41.2	14

Nomenclature: A, total surface area (m^2); **C,** fluid heat capacity (J /kg°C); **Cp,** pressure drop coefficient; D_o, outside diameter of tube (m); ***f*,** friction factor; **h,** heat transfer coefficient (W/m^2°C); **j,** Colburn factor; **k,** thermal conductivity (W/m°C); **Lp,** louver pitch (m); **Nu,** local Nusselt number, hD_o/k; $\overline{Nu}$ **,** average Nusselt number; **P,** pressure (Pa); **Pr,** Prandtl number, v/α; **q,** heat flux (W/m^2); **Re_D,** Reynolds numbers, $U_{max}D_o/v$; **T,** temperature (°C); **T_w,** wall temperature (°C); **T_{in},** inlet temperature (°C); **T_b,** bulk mean temperature (°C); **U_{in},** frontal velocity (m/s); **U_{max},** air velocity at minimum flow area (m/s); **x,y,z,** coordinates; **α,** thermal diffusivity (m^2/s); **θ,** louver angle (degree); **v,** kinematic viscosity (m^2/s); **ρ,** density of fluid (kg/m^3); **μ,** dynamic viscosity (kg/ms).

REFERENCES

Achaichia A, Cowell TA (1988). Heat transfer and pressure drop characteristics of flat tube and louvered plate fin surfaces, Experimental Thermal Fluid Sci. 1:147-157.
ANSYS FLUENT (2009). A Release 12.0, Documentation for ANSYS Workbench. ANSYS Ltd.
Chen YS, Kim SW (1987). Computation of Turbulent Flows Using an Extended K - ε turbulence Closure Model NASA CR-179204.

Davenport CJ (1983). Correlations for heat transfer and flow friction characteristics of louvred fin, AIChE Symposium Series. 19-27.

Hiramatsu M, Ishimaru T, Matsuzaki K (1990). Research on fins for air conditioning heat exchangers. JSME Int. J. Ser. II, 33:749-756.

Hsieh CT, Jang JY (2006). 3-D thermal-hydraulic analysis for louver fin heat exchangers with variable louver angle. Appl. Thermal Eng. 26:1629–1639.

Hsieh CT, Jang JY (2012). Parametric study and optimization of louver finned-tube heat exchangers by Taguchi method, Appl.Thermal Eng. 42:101-110.

Ikuta S, Sasaki Y, Tanaka K, Takagi M, Himeno R (1990). Numerical analysis of heat transfer around louver assemblies. Int. Congress & Exposition Tech., Detroit, Michigan, USA.

Jang JY, Shieh KP, Ay H (2001). 3-D thermal-hydraulic analysis in convex louver finned -tube heat exchangers, ASHRAE Annual Meeting, Cincinnati, OH, USA, June 22-27, pp. 501-509.

Jang JY, Tsai YC (2011). Optimum Louver Angle Design for a Louvered Fin Heat Exchanger, Int. J. Phys. Sci. 6:6422-6438.

Kays WM, London AL (1950). Heat transfer and flow friction characteristics of some compact heat exchanger surfaces-part I: test system and procedure, Trans. ASME 72:1075-1085.

Liakopoulos A (1984). Explicit representation of the complete velocity profile in a turbulent boundary layer, AIAA J. 22:844-846.

Sahnoun A, Webb RL (1992). Prediction of heat transfer and friction for louver fin geometry, ASME Journal of Heat Transfer 114:893-900.

Suga K, Aoki H, Shinagawa T (1990). Numerical analysis on two dimensional flow and heat transfer of louvered fins using overlaid grids. JSME Int. J. Ser. II, 33:122-127.

Suga K, Aoki H (1991). Numerical study on heat transfer and pressure drop in multilouvered fins. In Proceed. of ASME/JSME Thermal Eng. Joint Conf. 4:361-368.

Sunden B, Svantesson J (1992). Correlation of j- and f- Factors for multilouvered heat transfer surfaces. In proceedings of the 3rd UK National Heat Transfer Conf. 805-811.

Wang CC, Chi KY, Chang YJ (1998). An experimental study of heat transfer and friction characteristics of typical louver finned-tube heat exchangers, Int. J. Heat Mass Transfer. 41:817-822.

Wang TS, Chen YS (1993). Unified Navier-Stokes flowfield and performance analysis of liquid rocket engines, AIAA J. 9:678-685.

Webb RL (1994). Principles of Enhanced Heat Transfer, New York, John Wiley & Sons.

academicJournals

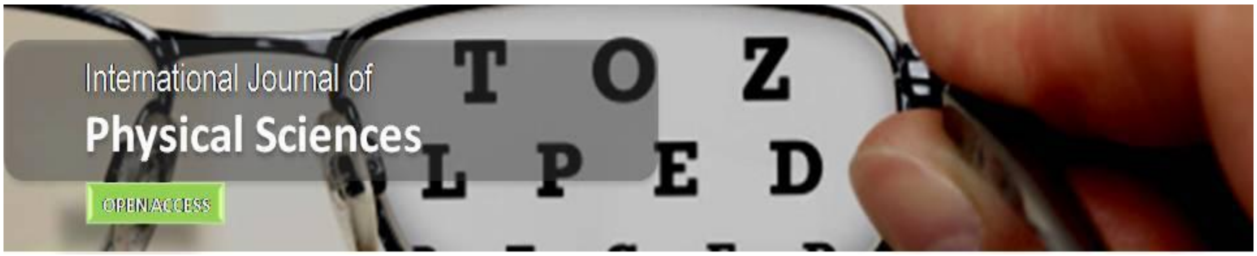

Related Journals Published by Academic Journals

- ■African Journal of Pure and Applied Chemistry
- ■Journal of Internet and Information Systems
- ■Journal of Geology and Mining Research
- ■Journal of Oceanography and Marine Science
- ■Journal of Environmental Chemistry and Ecotoxicology
- ■Journal of Petroleum Technology and Alternative Fuels